Original Article

MOLECULAR METABOLISM

Developmental metformin exposure does not rescue physiological impairments derived from early exposure to altered maternal metabolic state in offspring mice

Lídia Cantacorps[1,2], Jiajie Zhu[1], Selma Yagoub[1], Bethany M. Coull[1], Joanne Falck[1], Robert A. Chesters[1], Katrin Ritter[1], Miguel Serrano-Lope[1], Katharina Tscherepentschuk[1], Lea-Sophie Kasch[1], Maya Paterson[1], Paula Täger[1], David Baidoe-Ansah[1], Shuchita Pandey[1], Carla Igual-Gil[4], Annett Braune[5], Rachel N. Lippert[1,2,3,*]

ABSTRACT

Objective: The incidence of gestational diabetes mellitus (GDM) and metabolic disorders during pregnancy are increasing globally. This has resulted in increased use of therapeutic interventions such as metformin to aid in glycemic control during pregnancy. Even though metformin can cross the placental barrier, its impact on offspring brain development remains poorly understood. As metformin promotes AMPK signaling, which plays a key role in axonal growth during development, we hypothesized that it may have an impact on hypothalamic signaling and the formation of neuronal projections in the hypothalamus, the key regulator of energy homeostasis. We further hypothesized that this is dependent on the metabolic and nutritional status of the mother at the time of metformin intervention. Using mouse models of maternal overnutrition, we aimed to assess the effects of metformin exposure on offspring physiology and hypothalamic neuronal circuits during key periods of development.

Methods: Female C57BL/6N mice received either a control diet or a high-fat diet (HFD) during pregnancy and lactation periods. A subset of dams was fed a HFD exclusively during the lactation. Anti-diabetic treatments were given during the first postnatal weeks. Body weights of male and female offspring were monitored daily until weaning. Circulating metabolic factors and molecular changes in the hypothalamus were assessed at postnatal day 16 using ELISA and Western Blot, respectively. Hypothalamic innervation was assessed by immunostaining at postnatal days 16 and 21.

Results: We identified alterations in weight gain and circulating hormones in male and female offspring induced by anti-diabetic treatment during the early postnatal period, which were critically dependent on the maternal metabolic state. Furthermore, hypothalamic agouti-related peptide (AgRP) and proopiomelanocortin (POMC) neuronal innervation outcomes in response to anti-diabetic treatment were also modulated by maternal metabolic state. We also identified sex-specific changes in hypothalamic AMPK signaling in response to metformin exposure.

Conclusion: We demonstrate a unique interaction between anti-diabetic treatment and maternal metabolic state, resulting in sex-specific effects on offspring brain development and physiological outcomes. Overall, based on our findings, no positive effect of metformin intervention was observed in the offspring, despite ameliorating effects on maternal metabolic outcomes. In fact, the metabolic state of the mother drives the most dramatic differences in offspring physiology and metformin had no rescuing effect. Our results therefore highlight the need for a deeper understanding of how maternal metabolic state (excessive weight gain versus stable weight during GDM treatment) affects the developing offspring. Further, these results emphasize that the interventions to treat alterations in maternal metabolism during pregnancy need to be reassessed from the perspective of the offspring physiology.

Keywords Metformin; Gestational diabetes; Brain; Hypothalamus; Development; Metabolism

[1]Department of Neurocircuit Development and Function, German Institute of Human Nutrition Potsdam-Rehbruecke, Nuthetal, Germany [2]German Center for Diabetes Research (DZD), München-Neuherberg, Germany [3]NeuroCure Cluster of Excellence, Charité-Universitätsmedizin, Berlin, Germany [4]Department of Physiology of Energy Metabolism, German Institute of Human Nutrition Potsdam-Rehbruecke (DIfE), Nuthetal, Germany [5]Research Group Intestinal Microbiology, German Institute of Human Nutrition Potsdam-Rehbruecke, Nuthetal, Germany

*Corresponding author. Neurocircuit Development and Function (NDF), German Institute of Human Nutrition Potsdam-Rehbruecke, Arthur-Scheunert-Allee 114-116, 14558 Nuthetal, Germany. E-mail: Rachel.Lippert@dife.de (R.N. Lippert).

Received November 14, 2023 • Revision received December 18, 2023 • Accepted December 20, 2023 • Available online 23 December 2023

https://doi.org/10.1016/j.molmet.2023.101860

Abbreviations

ACC	acetyl-CoA carboxylase
AgRP	agouti-related peptide
AMPK	AMP-activated protein kinase
ARH	arcuate nucleus of the hypothalamus
BBB	blood—brain barrier
BSA	bovine serum albumin
CD	control diet
GDF15	growth differentiation factor 15
GDM	gestational diabetes mellitus
GWG	gestational weight gain
HFD	high-fat diet
HOMA-IR	homeostatic model assessment for insulin resistance
LKB1	liver kinase B1
Mate1	multidrug and toxic extrusion 1
MRL	Max-Rubner Laboratory
mTOR	mammalian target of rapamycin
mTORC1	mTOR complex 1
NPY	neuropeptide-Y
Oct	organic cation transporter
P	postnatal day
PBS	phosphate-buffered saline
PCOS	polycystic ovary syndrome
PFA	paraformaldehyde
PI3K	phosphatidylinositol 3-kinase
POMC	proopiomelanocortin
PVH	paraventricular nucleus of the hypothalamus
ROI	region of interest
RP	reversed-phase
RT	room temperature
SEM	standard error of the mean
SGA	small for gestational age
TBS-T	Tris-buffered saline containing 0.1% Tween-20
UK	United Kingdom

1. INTRODUCTION

Maternal gestational diabetes mellitus (GDM) rates continue to rise worldwide, affecting as many as one in six pregnancies. The global prevalence of GDM in 2021 was 14% [1] and interestingly it was high both in low- and high-income countries (12.7% and 14.2%, respectively). In Europe, the overall prevalence of GDM is estimated at around 10.9%, displaying a consistently increasing trend in most countries, such as Germany, with more than 50,000 cases documented in 2018 [2,3]. These high rates of GDM are of special concern, since glucose intolerance during pregnancy negatively affects both the mother's and the baby's health [4]. *In utero* exposure to hyperglycaemia is associated with impaired glucose metabolism in childhood [5] and increased offspring adiposity [6]. This increases the risk of developing obesity in later life, a phenomenon known as developmental programming.

Treatment options for GDM are relatively limited and their molecular side effects are not completely understood. Initial intervention relies on lifestyle changes related to diet and exercise [7]. If this is insufficient to normalize maternal glycemia, treatment with insulin therapy is typically prescribed. Critically, insulin itself does not cross the placental barrier [8,9], and the resulting positive effects on the foetus generally result from reducing the maternal blood glucose levels and subsequent fetal glycemia. However, in recent years, the development of oral antidiabetic therapeutics has led to their potential use for the treatment of GDM. The use of the oral biguanide metformin as a first line therapy has dramatically increased in the last years, with more than 85% of GDM pregnancies opting for metformin at first diagnosis in the United Kingdom (UK) [10]. Treatment with metformin prior to intervention with insulin is already accepted in the UK (https://www.nice.org.uk/guidance/ng3) [11], and its use in special cases as an off-label prescription is suggested in Germany [12]. This is prompted by current clinical evidence suggesting comparable safety between metformin and insulin on maternal and neonatal outcomes [13], although primary outcomes with metformin treatment were not superior to placebo [14] and there is still limited knowledge of the long-term consequences to the offspring.

Unlike insulin, metformin can cross the placenta [15,16] and can reach the fetus with similar levels as seen in maternal circulation. However, studies on the effects of intrauterine metformin exposure on offspring metabolic health are limited. Clinical studies have shown that children exposed to metformin *in utero* have more subcutaneous fat at the upper arm at 2 years of age [17] and are larger by measures of weight, arm and waist circumferences and BMI at 7—9 years of age when compared to insulin-exposed children [18]. Recently, maternal metformin treatment has been associated with a higher BMI in 9-year-old boys [19] [—] [21], thus suggesting a potential adverse effect of metformin exposure to offspring metabolic health. In addition, studies in pregnant people with polycystic ovary syndrome (PCOS) on metformin therapy have reported an increased body weight and BMI in 6-month-old children which persisted until 4 years of age [22], alongside an increased obesity risk in metformin-exposed children [23]. Moreover, an increased risk of being born small for gestational age (SGA) [24] was also observed in children with prenatal metformin exposure. Altogether, these data suggest a potential developmental programming role for metformin, as highlighted in recent reviews [25,26].

Animal studies of maternal metformin exposure recapitulate some of the findings observed in humans, although some opposing findings have been reported. A lower birthweight but increased offspring weight and fat accumulation when exposed to a high-fat diet (HFD) later in life was found when metformin was administered to pregnant dams on a regular diet [27]. However, when metformin was administered to diet-induced obese dams it had a protective effect on the offspring metabolic phenotype [28]. Furthermore, gestational metformin intervention in obese pregnant mice increased adiposity in adult male offspring [29] and did not prevent obesity-related changes in the fetus or the placenta [30]. However, other studies reported that metformin exposure during gestation or during lactation alone, on chow-fed dams, had an ameliorating effect on glucose tolerance in adult male mouse offspring by increasing their beta-cell insulin secretion [31,32]. Similarly, maternal metformin treatment had a protective effect against lactational-HFD metabolic liver defects in male offspring [33]. Lactational metformin has also been shown to reduce the weight of pups born to chow-fed mothers. However metformin could not rescue the lactational HFD-induced increase in body weight and adiposity [34]. Still, there is a lack of studies assessing the impact of maternal metformin exposure on offspring's brain physiology, thus highlighting the need for additional studies on this topic.

One of the main targets of metformin's action is AMP-activated protein kinase (AMPK) signaling, the consequences of which are still to be

elucidated in the developing brain. Amongst its actions, AMPK signaling directs axonal growth during development. AMPK activation prevents phosphatidylinositol 3-kinase (PI3K) transport to the neuronal growth cone resulting in a lack of neurite specification and polarization [35]. Furthermore, AMPK overactivation inhibits axonal outgrowth in hippocampal [36] and cortical neurons [37], thus demonstrating its ability to regulate neuronal structure.

The hypothalamus is the main brain center involved in the regulation of body energy homeostasis. The neuronal connectivity in the hypothalamus is established during the first postnatal weeks in mice [38]. Specifically, agouti-related peptide (AgRP) and proopiomelanocortin (POMC) axonal projections originating in the arcuate nucleus of the hypothalamus (ARH) develop from postnatal day (P) 6 and reach all their target hypothalamic nuclei by P18 [39]; a timepoint whereby hypothalamic nuclei resemble their adult structure. Thus, the perinatal period is a critical developmental window in which environmental factors, such as maternal nutrition, may alter neuronal development that subsequently lead to physiological changes in the offspring that could predispose them to metabolic disorders [40]. As previously reported in mouse models, AgRP and POMC hypothalamic innervation patterns can be disrupted by maternal HFD intake during lactation [41] and by maternal high-fat-high-sucrose diet during both pregnancy and lactation [42]. Further, genetic alterations to AMPK signaling, specifically in POMC and AgRP neurons, can also alter metabolic responses [43]. Interestingly, maternal nutritional state is also associated with changes in hypothalamic development in humans [44,45]. However, how exposure to anti-diabetic drugs during this critical developmental period influences the formation of neuronal circuits, and subsequent offspring metabolic regulation, is still to be clarified.

In this study, we hypothesized that metformin exposure, during the early postnatal period, impacts the development of hypothalamic neuronal circuits by altering AMPK signaling in the developing brain, which may result in long-lasting effects on brain function and whole-body energy homeostasis. We aimed to test this hypothesis in the context of maternal obesity and maternal gestational weight gain models, as both conditions contribute to the development of GDM but may result in different outcomes to the mother and offspring. Indeed, we show that the offspring response to anti-diabetic treatment is dependent on the maternal metabolic state in a sex-specific manner. Using a targeted nutritional intervention paired to specific periods of brain development we show a unique interaction of metformin treatment with maternal metabolic state on physiological outcomes in the offspring. Pharmacological treatment for GDM is usually prescribed considering maternal glycemic parameters during pregnancy, however, our results suggest that pre-pregnancy metabolic conditions can determine anti-diabetic treatment effects in the offspring.

2. MATERIAL AND METHODS

2.1. Mouse model

All mice were bred at an on-site animal facility at the Max-Rubner Laboratory (MRL) at the German Institute for Human Nutrition Potsdam-Rehbruecke (DIfE). Mice were housed in individually ventilated cages (IVC) cages with *ad libitum* access to food (unless otherwise stated) and sterile non-acidified water with a 12-hour on/off light cycle and constant room temperature (22 $\pm$ 2 °C). All experiments were approved by the competent authorities (Landesamt für Arbeitsschutz, Verbraucherschutz und Gesundheit; animal ethics application number 2347-7-2021) and were conducted in compliance with the ARRIVE guidelines and the European Directive 2010/63/EU.

Wild-type C57BL6/N male and female mice (Charles River, Strain #027) were used for postnatal hypothalamic tissue collection for the qPCR studies across development. Wild-type C57BL6/N female mice, as well as Rosa26-LSL-TdTomato (Jackson Laboratory, strain #007905) female mice maintained on a C57BL6/N background, were used for all maternal exposure experiments. At 4 weeks of age, after a week of acclimation to housing conditions, female mice were housed in pairs and fed either a control diet (CD) (#EF D12450B LS, Ssniff) or a high-fat diet (HFD) (#EF D12492, Ssniff) for 8 weeks before mating. The CD contained 67% kcal/carbohydrates, 13% kcal/fat and 20% kcal/proteins while the HFD contained 21% kcal/carbohydrates, 60% kcal/fat and 19% kcal/protein. Food intake and body weight were monitored weekly and water intake was ensured by weekly refilling of the water bottles. After 7 weeks, females were fasted overnight for 16 h to assess HOMA-IR. Those HFD-exposed females whose HOMA-IR was two standard deviations below the mean of all HFD-fed females were excluded from the study.

At 12 weeks of age, wild-type or TdTomato$^{loxp/loxp}$ females were mated with age-matched wild-type or Agrp-Cre/Pomc-Cre expressing males to produce AgRP^{tdTomato} or POMC^{tdTomato} offspring, respectively. The same diet was kept throughout gestation and food intake and body weight were measured every two days. Upon parturition (here defined as P0), half of the mothers receiving CD were switched to HFD (CD/HFD), while the other half of the mothers receiving CD were kept on CD (CD/CD). The HFD-fed dams were kept on HFD during lactation as well (HFD/HFD). Maternal body weight, food intake and water intake were daily measured during the lactation period. Litter size was adjusted to 5—8 pups per litter at postnatal days 0—1. Offspring were sacrificed at P16 or P21 with a minimum of 3 litters represented in each group.

AgRP^{tdTomato} or POMC^{tdTomato} offspring mice were ear-snipped at P14 and genotyped by PCR using the following primers: AgRP-IRES-Cre (common forward 5′-GATTACCCAACCTGGGCAGAAC-3'; wildtype reverse 5′-GGGCCCTAAGTTGAGTTTTCCT-3′ and mutant reverse 5′-GGGTCGCTACAGACGTTGTTTG-3′), *Pomc*-cre (common forward 5′-TGGC TCAATGTCCTTCCTGG-3'; wildtype reverse 5′- CACATAAGCTGCATCG TTAAG-3′ and mutant reverse 5′- GAGATATCTTTAACCCTGATC-3′) and LSL-TdTomato (wildtype forward 5′-AAGGGAGCTGCAGTGGAGTA-3'; wildtype reverse 5′-CCGAAAATCTGTGGGAAGTC-3'; mutant forward 5′-CTGTTCCTGTACGGCATGG-3′ and mutant reverse 5′-GGCATTAAAG-CAGCGTATCC-3′). The cycling conditions used were: step 1: 95 °C for 5 min; step 2: 95 °C for 30 s; step 3: 64 °C for AgRP-cre, 56 °C for POMC-cre or 61 °C for LSL-TdTomato for 30 s; step 4: 72 °C for 1 min (steps 2—4 repeated for 35 cycles); step 5: 72 °C for 5 min. PCR products were separated on a 1% agarose gel.

2.2. Anti-diabetic treatment administration

As depicted in Figure 1A, pharmacological interventions took place during the lactation phase starting from P4 to P21, matching the early postnatal period in which the hypothalamic neuronal projections are established, which in mice represents a time window opportunity for intervention. Treatments were given daily in the afternoon prior to onset of the dark phase. Lactating females were randomly split into three groups: vehicle, insulin and metformin, although in AgRP^{tdTomato} and POMC^{tdTomato} cohorts no insulin treatment group was included. The metformin-treated group consisted of dams receiving metformin hydrochloride (HCl) (#FM25131, Biosynth Carbosynth) into the drinking water (3 mg/ml) and the offspring were daily injected with metformin (200 mg/kg; i.p.), to ensure that they receive a similar dose of metformin as they would get *in utero*, as previous studies have shown the metformin levels reaching into the pups' circulation through the breast milk are almost undetectable [32]. The dose of metformin was chosen

based on previous studies [32] to reach an equivalent concentration in circulating blood to humans who have a prescribed metformin dose of 2 g/day. The insulin-treated group consisted of dams receiving an i.p. injection of 10 UI/kg long-acting insulin (100 UI/mL; Huminsulin basal, PZN #02526491, Lilly), calculated to reflect the dosage of 0.8 UI/kg/day used in pregnant humans [46] based on the allometric body surface method [47], and pups received saline injections (10 μl/g; i.p.). The control group (vehicle) of dams had access to autoclaved non-acidified drinking water and pups received daily saline injections (10 μl/g; i.p.) as a control intervention for i.p. injections. Thus, experimental offspring generated were divided into nine groups: gestational and lactational CD + vehicle (CD/CD/VEH), gestational and lactational CD + insulin (CD/CD/INS), gestational and lactational CD + metformin (CD/CD/MET), gestational CD and lactational HFD + vehicle (CD/HFD/VEH), gestational CD and lactational HFD + insulin (CD/HFD/INS), gestational CD and lactational HFD + metformin (CD/HFD/MET), gestational HFD and lactational HFD + vehicle (HFD/HFD/VEH), gestational HFD and lactational HFD + insulin (HFD/HFD/INS) and gestational HFD and lactational HFD + metformin (HFD/HFD/MET).

2.3. HOMA-IR determination

Tail blood was collected from fasted female mice in EDTA-coated tubes (#16,444, Sarstedt) and glucose levels were measured using a glucometer (Contour Care, Ascensia). Blood was centrifuged at 2,500 *g* for 20 min at 4 °C and supernatant was stored at −80 °C. Plasmatic insulin levels were determined using the Ultra-sensitive mouse insulin ELISA kit (#90082, Lot# 21APUMI623A, Crystal Chem). The HOMA-IR was then calculated as: [fasting insulin levels (μU/mL) x fasting glucose levels (mg/dL)/405].

2.4. Tissue collection

Mouse offspring were sacrificed at the same time of day on P16 or P21. Mice were transcardially perfused with ice-cold phosphate-buffered saline (PBS) followed by 4% paraformaldehyde (PFA) in borate buffer (pH 9.5) (#441244, Sigma–Aldrich) under deep anaesthesia using pentobarbital (400 mg/kg; i.p.) diluted in isotonic sodium chloride solution (#1021010, Deltamedica). Whole brains were harvested, postfixed for 4 h in 4% PFA and cryoprotected in 20% sucrose in PBS overnight at 4 °C. The brains were then frozen and stored at −80 °C until further processing.

Cre-negative mouse offspring were sacrificed at P16 by decapitation and brain regions were freshly dissected, snap-frozen on dry ice and stored at −80 °C. Blood glucose levels were determined from trunk blood using a glucometer (Contour Care, Ascensia).

2.5. Quantification of plasma hormone levels

Trunk blood from P16 offspring was collected in EDTA-containing tubes. After centrifugation at 2,500 g for 20 min at 4 °C, plasma was aliquoted and stored at −80 °C. Insulin levels were determined using the Ultra-sensitive mouse insulin ELISA kit (#90082, Lot 21APUMI623A, Crystal Chem), leptin levels were measured using the Mouse Leptin ELISA kit (#90030, Lot 21OCML444, Crystal Chem), total ghrelin was quantified using the Rat/Mouse Ghrelin (Total) ELISA Kit (#EZRGRT-91K, Lot 3799697, Millipore), and GDF15 levels were measured using the mouse/rat GDF-15 quantikine ELISA kit (#MGD1500, R&D systems) according to the manufacturer's procedure guidelines. A SPECTROstar Nano microplate reader (BMG labtech) was used to measure absorbance.

2.6. AgRP and α-MSH fiber density measurement

Frozen brains from P16 and P21 wild-type progeny were cut into 30 μm-thick coronal sections using a sliding microtome (#400410, Slide 4004 M, pfm medical) and serial sections were stored at −20 °C in glycerol-containing PBS solution until further use. Brain sections including the hypothalamus were first permeabilized with 0.3% glycine and 0.03% SDS for 10 min each and blocked with 0.125% Triton-X and 3% normal donkey serum in K-PBS for 1 h at room temperature (RT). Sections were then immunostained with rabbit anti-mouse AgRP antibody (1:4,000, #H-003-53, Phoenix Pharmaceuticals) and sheep anti-mouse α-MSH antibody (1:40,000, #AB5087, Merck) in SignalStain solution (#8112, Cell Signaling) for 72 h at 4 °C. Next, the slices were incubated with Alexa Fluor 488 donkey anti-rabbit (1:1,000, #A21206, Invitrogen) and Alexa Fluor 633 donkey anti-sheep (1:1,000, #A21100, Invitrogen) antibodies for 1 h at RT. Finally, stained slices were mounted and coverslipped with Vectashield Antifade mounting medium containing DAPI (#VEC-H-1200, Biozol).

Representative sections of the anterior PVH (from bregma −0.83 mm to −0.95 mm) and the posterior PVH (from bregma −1.07 to −1.23 mm) of each animal were imaged by a blinded experimenter to the groups using 16 z-stacks with an optimal thickness of 1.5 μm. Images were acquired on a Zeiss confocal microscope equipped with a 20× objective. Image quantification analysis was performed using ImageJ software v2.1.0 (National Institute of Health). First, z-stacks were compressed into a single plane on the z-axis using the maximum intensity projection function and a region of interest (ROI) was manually drawn around the limits of the anatomical region. Then, the tissue background signal was removed by subtracting the mode value based on the histogram of signal intensity obtained for each image channel and the resultant image was thresholded and converted to a binary image. Next, the area containing immunostained pixels was measured and divided by the total area of the analysed ROI to obtain the percentage of stained area as an indicator of labeled fiber density. If multiple sections were present in the correct region for each animal, the average percentage of area was calculated. Data were then normalised to the mean of the control group (CD/CD/VEH).

2.7. POMC and AgRP neuronal cell count

Frozen brains of AgRP^{tdTomato} or POMC^{tdTomato} P16 mice were sliced into 30 μm-thick coronal sections using a sliding microtome (#400410, Slide 4004 M, pfm medical) and serial sections were stored in glycerol-containing PBS solution at −20 °C until further use. Brain sections including the hypothalamus were first permeabilized with 0.3% glycine and 0.03% SDS for 10 min each and blocked with 0.125% Triton-X and 3% normal donkey serum in K-PBS for 1 h at RT. For AgRP^{tdTomato}, slices were immunostained with rabbit anti-mouse AgRP antibody (1:4,000, #H-003-53, Phoenix Pharmaceuticals) and goat anti-TdTomato antibody (1:4,000, #AB8181-200, Sicgen), while slices of POMC^{tdTomato} were incubated with sheep anti-mouse α-MSH antibody (1:40,000, #AB5087, Merck) and goat anti-TdTomato antibody (1:4,000, #AB8181-200, Sicgen) in SignalStain solution (#8112, Cell Signaling) for 72 h at 4 °C. Then, the slices were incubated either with Alexa Fluor 488 donkey anti-rabbit (1:1,000, #A21206, Invitrogen) or Alexa Fluor 488 donkey anti-sheep (1:1,000, #A11015, Invitrogen) secondary antibodies for labelling AgRP or α-MSH, respectively; and Alexa Fluor 633 donkey anti-goat (1:1,000, #A21082, Invitrogen) secondary antibody for TdTomato labelling for 1 h at RT. Finally, stained slices were mounted and coverslipped with Vectashield Antifade mounting medium containing DAPI (#VEC-H-1200, Biozol).

16 z-stacks of 1.5-μm optical thickness of representative sections of the rostral ARH (from bregma 1.31 mm to −1.55 mm) and mid ARH (from bregma −1.67 mm to −1.97 mm) of each animal were acquired using a Zeiss confocal microscope equipped with a 20× objective. Neuronal cell counts were performed using ImageJ software v2.1.0/1.53 g (National Institute of Health) and in-house macros to automatically detect and count tdTomato + cells. First, z-stacks were converted into maximum intensity projection images. Then, each image was binarized using FIJI's Moments threshold algorithm and images were segmented using "despeckle" and "watershed" plugins to define individual cells. For automated cell number counting within each manually drawn ROI, the "Analyze particles" command was run with the following criteria: circularity of 0.10—1.0, size from 40 μm^2 to infinity. For quality control, all images were checked afterwards and tdTomato-positive cells were also manually counted.

2.8. Analysis of protein expression by Western Blot

Hypothalamus samples were homogenized in RIPA lysis buffer in the presence of protease (#5892970001, EASYpack, Roche) and phosphatase (#4906837001, PhosSTOP, Roche) inhibitors and centrifuged at 15,808 *g* for 20 min at 4 °C. Total levels of protein were determined using the Pierce BCA assay kit (#23225, Thermo Fisher). Twelve μg of protein suspended in 5× loading buffer was separated by SDS-polyacrylamide gel electrophoresis (10% gels) and then transferred to PVDF membranes (#IPVH00005, Immobilon-P, Merck). Membranes were blocked with 5% bovine serum albumin (BSA) in Tris-buffered saline containing 0.1% Tween-20 (TBS-T) for 1 h at RT and then primary antibodies (Table 1) diluted in TBS-T were incubated overnight at 4 °C, followed by incubation with IRDye 680 goat anti-rabbit (#611-144-022, Rockland) and IRDye 800 goat anti-mouse (#610-145-121, Rockland) secondary antibodies for 1 h in the dark at RT. Detection of fluorescence bands was carried out on an Odyssey Infrared Imaging Scanner (LI-COR Biosciences) and relative protein expression was quantified using Image Studio Lite software.

2.9. Determination of serum metformin levels by HPLC analysis

Metformin-treated dams were sacrificed after weaning by decapitation under isoflurane anaesthesia and trunk blood was collected. After centrifugation of blood samples at 2,500 *g* for 20 min at 4 °C, serum was stored at −80 °C. Metformin levels in serum were analysed by reversed-phase (RP) HPLC following a one-step protein precipitation protocol (adapted from Chhetri et al. [48]).

Table 1 — Antibodies used for Western Blot.

Antigen	Host	Dilution	Supplier	Catalog n°.
Acetyl-CoA carboxylase (ACC)	Rabbit	1:1000	Cell Signaling Technologies	#3662
AMPK-α	Rabbit	1:500	Cell Signaling Technologies	#2532
GAPDH	Mouse	1:2500	Santa Cruz Biotechnology	sc-365062
LKB-1	Rabbit	1:1000	Cell Signaling Technologies	#3047
mTOR	Rabbit	1:1000	Cell Signaling Technologies	#2972
phospho-Acetyl-CoA Carboxylase (Ser^{79})	Rabbit	1:1000	Cell Signaling Technologies	#3661
phospho-AMPKα (Thr^{172})	Rabbit	1:1000	Cell Signaling Technologies	#2535
phospho-LKB1 (Ser^{428})	Rabbit	1:1000	Cell Signaling Technologies	#3482
phospho-mTOR (Ser^{2448})	Rabbit	1:1000	Cell Signaling Technologies	#2971
β-Actin	Mouse	1:2500	Santa Cruz Biotechnology	sc-47778
β-Tubulin	Mouse	1:5000	BD Biosciences	#556321

Stock solutions (1 mM) of metformin HCl (#FM25131, Biosynth Carbosynth) and buformin HCl (#HY-B2099A, MedChemExpress) were prepared in distilled water. Buformin HCl was used as the internal standard. To determine the detection limit of metformin, untreated mouse serum samples were spiked with increasing concentrations of metformin (0.5—50 μM). Buformin aliquots (2.5 μl) were added to 117.5 μl of serum samples collected from metformin-treated dams to a final concentration of 20.8 μM. For protein precipitation, 5 μl perchloric acid (60%) was added and mixtures were centrifuged at 9,400 *g* for 3 min at 4 °C. An aliquot (20 μl) of the collected supernatants was used for HPLC analysis.

The HPLC system (Summit, Dionex, Idstein, Germany) was equipped with a pump (P 680A LPG-4), an autosampler (ASI-100T), a thermo stated column compartment (TCC-100) with eluent preconditioner, a photodiode array detector (UVD 340U), and a LiChrospher 100 RP-18 column (250 × 4 mm i.d., 5 μm) combined with a corresponding guard column (Merck, Darmstadt, Germany). The column temperature was kept at 30 °C. The mobile phase contained 34% acetonitrile and 66% of the aqueous phase composed of 10 mM potassium phosphate buffer, pH 5.2, and 10 mM sodium dodecyl sulfate. The flow rate was 1.3 ml min^{-1}. Detection was at 233 nm and UV spectra were recorded in the range of 200—400 nm. For control of the HPLC system and data processing, the Chromeleon software version 6.40 (Dionex, Sunnyvale, USA) was applied. Compounds were quantified based on calibration curves (5—100 μM). Metformin concentrations were calculated according to the percentage of recovery of the internal standard. The observed limit of detection of metformin in mouse serum was 5 μM.

2.10. Determination of gene expression by RT-qPCR

To determine the expression of metformin uptake transporters in the developing hypothalamus, male and female wild-type C57BL6/N mice born to standard chow-fed dams were sacrificed under isoflurane anaesthesia at different time points across postnatal development (P6, P9, P11, P14, P16, P21 and 8 weeks of age). The hypothalami were freshly dissected, snap frozen and stored at −80 °C. Total RNA from dissected hypothalamus was isolated with TRIzol reagent [38% phenol, 0.8 M guanidinium thiocyanate, 0.4 M ammonium thiocyanate, 0.1 M sodium acetate and 5% glycerol] and glycogen (#M6015.0005, Genaxxon bioscience). Chloroform (#102445, Merck) was used for phase separation and ice-cold isopropanol (#7343.1, Carl Roth) for RNA precipitation. After centrifugation at 7,600 g for 15 min at 4 °C, pellets were resuspended in 30 μl diethyl pyrocarbonate-treated water before adding DNase 10× buffer (#B43, Fisher Scientific), Superasin (#AM2696, Fisher Scientific) and DNase I (#EN0521, Fisher Scientific). RNA concentration was quantified using the Quantus Fluorometer (Promega). cDNA synthesis was performed using the NZY first-strand cDNA synthesis kit (#MB12502, NZYtech). Each PCR reaction (20 μl final volume) was run at 50 °C for 30 min, 85 °C for 5 min, 37 °C for 20 min and then kept at 4 °C. 5 ng of cDNA were used for quantitative real-time PCR (RT-qPCR) mixed with NZY Speedy qPCR Green Master Mix (#MB223, NZYtech) and 0.4 μM of primers in a total volume of 10 μl. Primer sequences used are shown in Table 2. Amplification was performed on Applied Biosystems QuantStudio 12K Flex real-time PCR system. Relative gene expression was calculated using the $2^{-\Delta\Delta Ct}$ comparative method after normalization to the P6 time-point. *Gapdh* was used as a housekeeping gene (Table 3).

2.11. Statistical analysis

All data are presented as mean ± standard error of the mean (SEM) with single data points except for the box plots where whiskers are min. to

Table 2 — Primer sequences used for RT-qPCR.

Gene	Forward (5′ to 3′)	Reverse (5′ to 3′)
Gapdh	CGACTTCAACAGCAACTCCCACTCTTCC	TGGGTGGTCCAGGGTTTCTTACTCCTT
Mate1 (also known as SLC47A1)	GCCATCGTTAATGCCATCGGGTA	CAGGCCGATCACTCCCAGCTT
Oct1 (also known as SLC22A1)	TTGGAGAGTTTGGCTGGTTC	CACCAGGAGGCAGAGCTTAC
Oct3 (also known as SLC22A3)	ATCCTGAGGCGCGTGGCTAA	GCGCTCGTGAACCAAGCAAACAT

max. overlaid with individual data points, the hinges of boxes represent the 25th and 75th percentiles, and the middle line is the median. When data are relativized, they are given as a percentage of the group control (CD/CD/VEH). Statistical analyses were performed using GraphPad Prism 9.2.0 (GraphPad software, La Jolla, CA, USA). Multiple groups were compared using one-way or two-way ANOVA analysis followed by Tukey's post hoc comparisons or two-way ANOVA with repeated measures followed by Bonferroni post-hoc comparisons when appropriate. Unpaired two-tailed Student's t-tests were used to compare between two groups. Correlations were calculated using Pearson's test. Significant differences were considered when p-value <0.05.

3. RESULTS

3.1. Timing of maternal HFD feeding and anti-diabetic treatments affect maternal metabolic state

Both gestational weight gain (GWG) and maternal obesity are risk factors for the development of GDM. In our study (Figure 1A), we used two different mouse models of maternal metabolic states during pregnancy and lactation by targeting specific developmental periods during early life to model both maternal obesity and excessive GWG. Female mice fed with HFD for 8 weeks prior to mating, during pregnancy and lactation were used as a model of maternal obesity. Another group of females had access to control diet (CD) prior to, and during gestation, and were switched to HFD at birth; resembling a model of excessive weight gain during the early postnatal developmental period. Pregnant people with GDM are generally diagnosed between gestational weeks 24–28 [49], and when required, pharmacological interventions are given during the third trimester of pregnancy. In the context of brain development, the lactation period in rodents is the equivalent period to the third trimester of human pregnancy [50]. Hence, in our study, we administered the anti-diabetic treatments insulin and metformin, as well as vehicle, from P4 until weaning to the female mice and their offspring.

Dams exposed to HFD for 8 weeks prior to pregnancy showed an increase in their body weight from the second week onwards (Supplementary Fig. 1A), as well as increased food consumption (kcal/day) during the 8-week pre-pregnancy period (Supplementary Fig. 1B; Supplementary Table 1). After 7 weeks, HFD-fed females displayed increased fasting blood glucose levels (Supplementary Fig. 1C), elevated plasma insulin concentrations ($p = 0.05$, Supplementary Fig. 1D) and an increase in the homeostatic model assessment for insulin resistance (HOMA-IR) (Supplementary Fig. 1E). This indicates an insulin resistant phenotype induced by HFD feeding prior to pregnancy. HFD-fed dams also consistently showed an increased body weight during pregnancy (Supplementary Fig. 1F). Notably, however, both CD- and HFD-fed dams gained weight in a similar fashion (Supp. Fig. 1G). During gestation, HFD-fed dams kept an elevated food intake (Supplementary Fig. 1H), although their caloric intake was normalized to that of CD-fed dams on the last days of pregnancy. There were no significant effects of maternal diet on litter size (Supplementary Fig. 1I) nor on the proportion of males and females per litter (Supplementary Fig. 1J).

Upon parturition, half of the mothers on CD were switched to HFD. Maternal body weight and food intake were monitored during the first three postnatal weeks in all groups to assess the effects of maternal diet on metabolic state. Maternal diet had a significant effect on maternal body weight across the postnatal period in all treatment groups as shown in Figure 1B,C and D (Table 3). Obese mothers (HFD/HFD) maintained a higher weight than CD/CD mothers, while CD/HFD dams displayed a dramatic increase in their body weight, reaching similar levels to HFD/HFD mothers. Specifically, CD/HFD females displayed an increased body weight gain from P1 to P16, independently of the treatment received (Figure 1E), thus resembling a model of excessive GWG. Regarding their food intake, there were no significant differences due to maternal diet on the vehicle-treated dams (Figure 1F), although a modest increase in caloric intake over time was significant in all groups of dams (Figure 1F,G and H). However, maternal diet had a different impact on food consumption in both insulin- and metformin-treated dams. Analysis of the cumulative food intake during the lactation period (Figure 1I) revealed a significant increase in food intake in the CD/HFD mothers exposed to metformin compared to the vehicle-treated mothers, as well as compared to the metformin-treated CD/CD and HFD/HFD mothers. This indicates that metformin exposure alone can promote food consumption in the CD/HFD mothers. Maternal HFD feeding either during lactation or throughout gestation and lactation induced elevated blood glucose levels in the mothers (Figure 1J). This was not rescued by anti-diabetic treatments. However, metformin exposure lowered circulating insulin levels in all groups of mothers (Figure 1K) and it also had a counteracting effect on the HFD-induced hyperleptinemia in the mothers (Figure 1L). In addition, we measured the circulating levels of growth differentiation factor 15 (GDF15) in the mothers, as it is considered a biomarker for the use of metformin [51]. Accordingly, elevated GDF15 levels were found in the groups of dams treated with metformin (Figure 1M). Furthermore, increased GDF15 levels in the mothers fed with HFD during lactation (CD/HFD) regardless of the treatment exposure were observed (Figure 1M).

In sum, maternal HFD exposure during the lactation period in mice induced excessive maternal weight gain whereas HFD feeding prior to pregnancy and throughout pregnancy and lactation induced a maternal obese phenotype during the first postnatal weeks. Anti-diabetic drugs did not affect maternal weight gain or end-point glycemia, but metformin lowered circulating insulin and leptin levels in the mothers. Thus, metformin treatment may be able to restore some of the maternal metabolic impairments induced by maternal HFD feeding.

3.2. Metformin in the drinking water leads to clinically relevant metformin circulating levels in the mothers

To confirm therapeutic levels of circulating metformin in the mothers, daily water intake was measured during the lactation period. Water

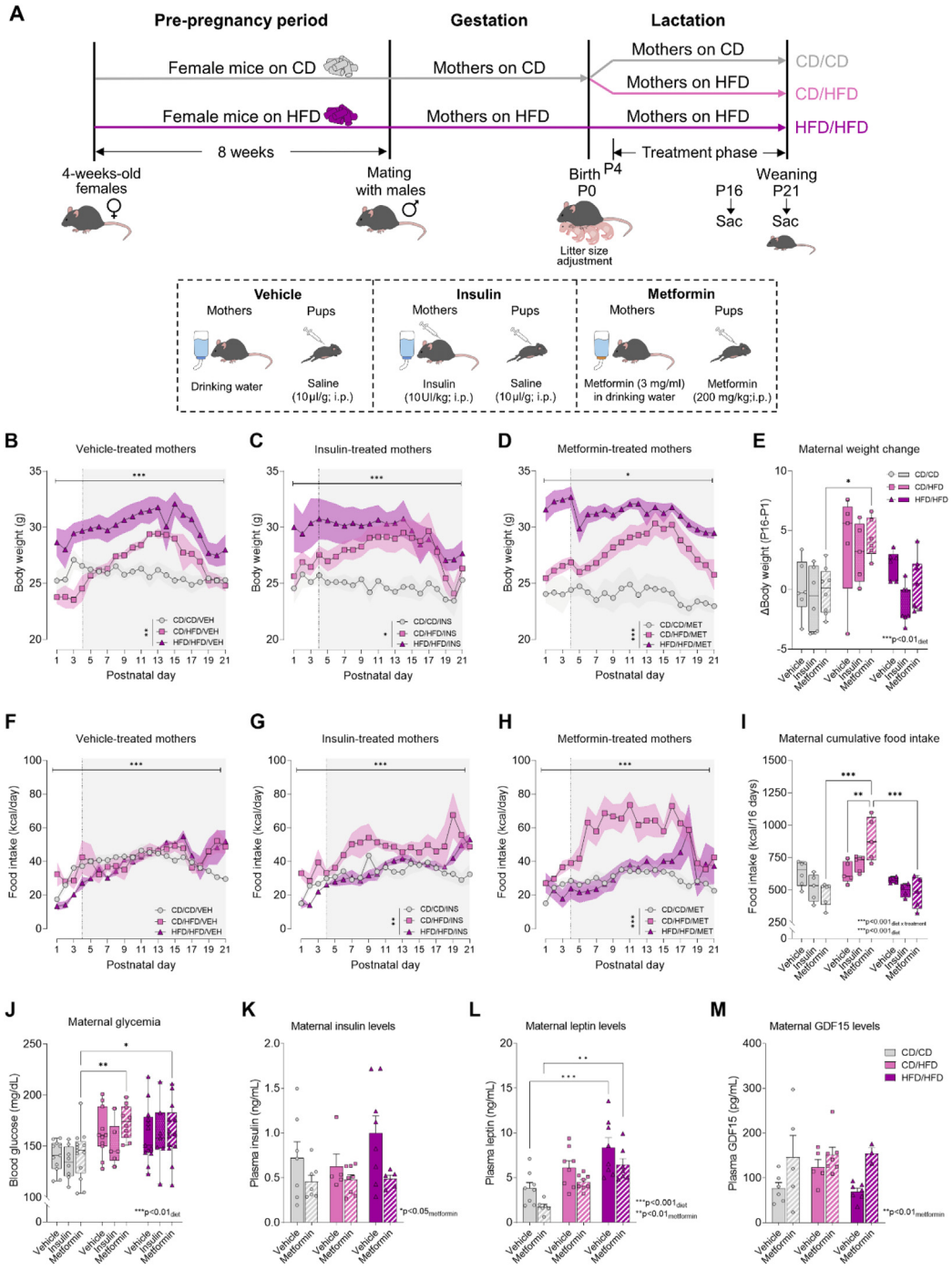

Figure 1: Maternal HFD intake during lactation leads to excessive maternal weight gain and hyperglycemia at weaning which is not affected by metformin treatment. (A) Schematic representation of experimental design for maternal dietary exposure, treatment interventions and offspring tissue collection at P16 or P21. (B–D) Maternal body weight throughout the lactation period in vehicle-treated, insulin-treated and metformin-treated mothers (n = 3–6/group). (E) Maternal body weight gain from P1 to P16 (n = 5–8/group). (F–H) Maternal food intake throughout the lactation period in vehicle-treated, insulin-treated and metformin-treated mothers (n = 4–6/group). (I) Maternal cumulative food intake from P1 to P16 (n = 4–6/group). (J) Maternal random blood glucose levels (mg/dl) at weaning (n = 6–13/group), (K) maternal circulating insulin levels (ng/ml) at weaning (n = 5–8/group), (L) maternal circulating leptin levels (ng/ml) at weaning (n = 6–8/group) and (M) GDF15 plasma levels (pg/ml) at weaning (n = 3–7/group). Light grey shadowed area represents treatment phase, connecting lines represent mean and SEM is represented as colour-specific surrounding fill area (B, C, D, F, G H). In data plotted as box plots (E, I, J) whiskers are min. to max., hinges of boxes are 25th and 75th percentiles, and the middle line is the median. In bar graphs (K, L, M), data are expressed as mean ± SEM with single data points. *$p < 0.05$, **$p < 0.01$, ***$p < 0.001$ derived from 2-way ANOVA with repeated measures (diet x time; B, D, F, H), mixed effects model (diet x time; C, G) or 2-way ANOVA followed by Tukey's multiple comparisons (diet x treatment; E, I, J, K, L). CD/CD: gestational and lactational control diet-fed mothers, CD/HFD: gestational control diet and lactational high-fat diet-fed mothers, HFD/HFD: gestational and lactational high-fat diet-fed mothers, P: postnatal day. Mouse and food icons are from https://scidraw.io/.

Table 3 — Two-way ANOVA results for Figure 1.

Panel	Source of variation	F (DFn, DFd)	P value
B) Body weight vehicle-treated mothers	Diet	F (2, 13) = 9.55	P = 0.003
	Time	F (4.91, 63.87) = 12.50	P < 0.001
	Diet x Time	F (42, 273) = 4.40	P < 0.001
C) Body weight insulin-treated mothers	Diet	F (2, 10) = 5.83	P = 0.021
	Time	F (3.43, 34.3) = 7.24	P < 0.001
	Diet x Time	F (42, 210) = 2.61	P < 0.001
D) Body weight metformin-treated mothers	Diet	F (2, 13) = 27.31	P < 0.001
	Time	F (3.56, 46.21) = 3.70	P = 0.014
	Diet x Time	F (42, 273) = 2.86	P < 0.001
E) Maternal weight change	Diet	F (2, 47) = 14.00	P < 0.001
	Treatment	F (2, 47) = 2.31	P = 0.111
	Diet x Treatment	F (4, 47) = 0.66	P = 0.625
F) Food intake vehicle-treated mothers	Diet	F (2, 12) = 0.75	P = 0.494
	Time	F (2.93, 35.10) = 11.54	P < 0.001
	Diet x Time	F (40, 240) = 2.68	P < 0.001
G) Food intake insulin-treated mothers	Diet	F (2, 9) = 6.88	P = 0.015
	Time	F (5.77, 51.90) = 17.99	P < 0.001
	Diet x Time	F (40, 180) = 2.97	P < 0.001
H) Food intake metformin-treated mothers	Diet	F (2, 13) = 17.44	P < 0.001
	Time	F (6.19, 80.49) = 7.61	P < 0.001
	Diet x Time	F (40, 260) = 2.70	P < 0.001
I) Maternal cumulative food intake	Diet	F (2, 36) = 22.70	P < 0.001
	Treatment	F (2, 36) = 0.85	P = 0.435
	Diet x Treatment	F (4, 36) = 6.37	P < 0.001
J) Maternal glycemia	Diet	F (2, 83) = 10.20	P < 0.001
	Treatment	F (2, 83) = 1.53	P = 0.223
	Diet x Treatment	F (4, 83) = 0.35	P = 0.841
K) Maternal insulin levels	Diet	F (2, 34) = 0.99	P = 0.382
	Metformin	F (1, 34) = 7.21	P = 0.011
	Diet x Metformin	F (2, 34) = 0.84	P = 0.441
L) Maternal leptin levels	Diet	F (2, 39) = 18.99	P < 0.001
	Metformin	F (1, 39) = 9.75	P = 0.003
	Diet x Metformin	F (2, 39) = 0.05	P = 0.950
M) Maternal GDF15 levels	Diet	F (2, 27) = 0.90	P = 0.417
	Metformin	F (1, 27) = 10.27	P = 0.003
	Diet x Metformin	F (2, 27) = 0.86	P = 0.433

intake significantly increased throughout the lactation period in all groups of lactating dams independently of the treatment group (Supplementary Figs. 2A, B, C; Supplementary Table 2), but only in metformin-treated dams there was an impact of maternal diet ($p < 0.01$). Analysis of the average daily water intake during lactation (Supplementary Figure 2D) revealed a significant effect of both *diet* and *treatment*, with a reduction in water intake due to anti-diabetic treatment, and an increased overall water consumption in the CD/HFD group of mothers. The estimated daily metformin intake calculated from water intake (Supplementary Fig. 2E) was higher in the CD/HFD group of mothers compared to the CD/CD group ($p < 0.01$), and the metformin dose calculated according to the water intake and body weight (Supplementary Fig. 2F) was higher in the CD/HFD mothers compared to HFD/HFD mothers ($p < 0.01$).

Critically, despite changes to overall maternal water intake due to metformin, the resulting effect on circulating metformin levels showed no difference between dietary intervention groups (Supplementary Fig. 2G). We therefore conclude that all groups of dams had a similar exposure to metformin. We could also show that metformin given in the drinking water elicits serum concentrations within the therapeutic range found in diabetic patients receiving 2 g/day of metformin [52]. Overall, there was a significant correlation between the average daily water intake during lactation and the maternal serum metformin concentrations (Supplementary Fig. 2H). Consistent with the known glucose lowering effect of metformin, maternal glucose levels correlated negatively with metformin serum levels (Supplementary Fig. 2I). Previous studies report almost undetectable levels of maternal circulating metformin in breast milk and offspring blood serum [32,53—55]. We therefore also administered metformin directly to the pups, to ensure that the offspring received equivalent doses of metformin, as would be seen in humans. Critically, our initial metformin dosage to the offspring (300 mg/kg) resulted in increased postnatal death (37%) and subsequent experiments were performed using a lower dose (200 mg/kg) of metformin treatment [56] which dramatically improved outcomes for pup survival (Supplementary Table 3).

3.3. Growth and physiological outcomes in offspring exposed to early overnutrition and pharmacological interventions are dependent on the maternal metabolic state

Both male and female offspring from HFD-fed mothers in the vehicle control group weighed less during the first postnatal days than CD/CD offspring (Figure 2A,K, Table 4). Whereas when exposed to anti-diabetic treatments (insulin or metformin) both male and female offspring from CD/HFD mothers showed higher body weights compared to offspring from CD/CD or HFD/HFD mothers. Furthermore, both insulin and metformin treatment seemed to cause a reduction in body weight in female offspring from obese mothers (HFD/HFD) compared to CD/CD female offspring across the early postnatal period. This effect was not observed in males (Figure 2B,C, L and M).

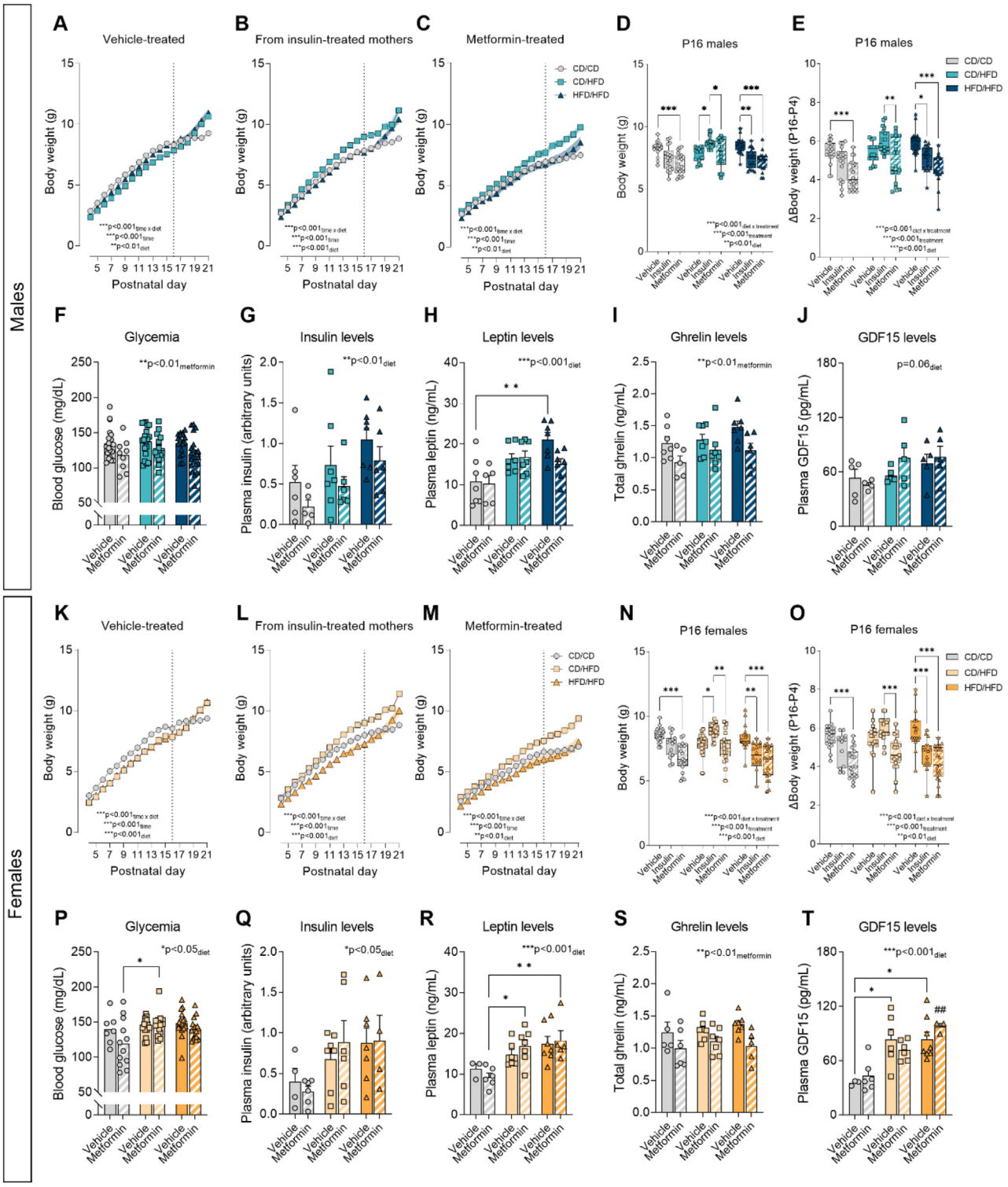

Figure 2: Anti-diabetic treatments effects on offspring growth and metabolic hormone levels is dependent on maternal metabolic state. (A—C) Male offspring body weight from vehicle-treated group, from insulin-treated mothers and from metformin-treated group from P4 to P21 (n = 11—14/group). (D) Male offspring body weight at P16 and (E) body weight change from P4 to P16 (n = 16—21/group). (F) Blood glucose levels (n = 18—20/group), (G) insulin, (H) leptin, (I) ghrelin and (J) GDF15 plasma levels in P16 male offspring (n = 5—7/group). (K—M) Female offspring body weight from vehicle-treated group, from insulin-treated mothers and from metformin-treated group from P4 to P21 (n = 10—14/group). (N) Female offspring body weight at P16 and (O) body weight changes from P4 to P16 (n = 16—21/group). (P) Blood glucose levels (n = 7—18/group), (Q) insulin, (R) leptin, (S) ghrelin and (T) GDF15 plasma levels in P16 female offspring (n = 3—7/group). Connecting lines represent mean and SEM is represented as colour-specific surrounding fill area, dotted line indicates P16 time-point (A, B, C, K, L, M). In data plotted as box plots (D, E, N, O) whiskers are min. to max., hinges of boxes are 25th and 75th percentiles, and the middle line is the median. In bar graphs (F, G, H, I, J, P, Q, R, S, T), data are expressed as mean ± SEM with single data points. *p < 0.05, **p < 0.01, ***p < 0.001 derived from 2-way ANOVA with repeated measures (diet x time; A, B, C, K, L, M) and 2-way ANOVA followed by Tukey's multiple comparisons (diet x treatment; D, E, F, G, H, I, J, N, O, P, Q, R, S, T), ##p < 0.01 compared to CD/CD/MET (T). CD/CD: gestational and lactational control diet-exposed, CD/HFD: gestational control diet and lactational high-fat diet-exposed, HFD/HFD: gestational and lactational high-fat diet-exposed.

Table 4 — Two-way ANOVA results for Figure 2.

Panel	Source of variation	F (DFn, DFd)	P value
A) Body weight vehicle group males	Diet	F (2, 36) = 5.34	P = 0.009
	Time	F (3.59, 129.3) = 1635	P < 0.001
	Diet x Time	F (34,612) = 15.37	P < 0.001
B) Body weight insulin-exposed males	Diet	F (2, 34) = 11.03	P < 0.001
	Time	F (4.12, 140) = 1279	P < 0.001
	Diet x Time	F (34, 578) = 8.73	P < 0.001
C) Body weight metformin-treated males	Diet	F (2, 31) = 6.17	P = 0.006
	Time	F (4.21, 130.6) = 656.90	P < 0.001
	Diet x Time	F (34, 527) = 6.49	P < 0.001
D) Body weight P16 males	Diet	F (2, 156) = 6.81	P = 0.001
	Treatment	F (2, 156) = 15.20	P < 0.001
	Diet x Treatment	F (4, 156) = 9.30	P < 0.001
E) Body weight change males	Diet	F (2, 158) = 9.88	P < 0.001
	Treatment	F (2, 158) = 25.20	P < 0.001
	Diet x Treatment	F (4, 158) = 4.92	P < 0.001
F) Glycemia P16 males	Diet	F (2, 94) = 0.87	P = 0.422
	Metformin	F (1, 94) = 10.21	P = 0.002
	Diet x Metformin	F (2, 94) = 0.22	P = 0.804
G) Insulin levels P16 males	Diet	F (2, 31) = 4.78	P = 0.016
	Metformin	F (1, 31) = 3.76	P = 0.062
	Diet x Metformin	F (2, 31) = 0.01	P = 0.989
H) Leptin levels P16 males	Diet	F (2, 34) = 10.45	P < 0.001
	Metformin	F (1, 34) = 2.11	P = 0.155
	Diet x Metformin	F (2, 34) = 2.25	P = 0.121
I) Ghrelin levels P16 males	Diet	F (2, 33) = 2.13	P = 0.135
	Metformin	F (1, 33) = 10.32	P = 0.003
	Diet x Metformin	F (2, 33) = 0.54	P = 0.586
J) GDF15 levels P16 males	Diet	F (2, 23) = 3.11	P = 0.064
	Metformin	F (1, 23) = 0.66	P = 0.423
	Diet x Metformin	F (2, 23) = 0.99	P = 0.384
K) Body weight vehicle group females	Diet	F (2, 37) = 11.44	P < 0.001
	Time	F (2.47, 91.48) = 1295	P < 0.001
	Diet x Time	F (34, 629) = 12.23	P < 0.001
L) Body weight insulin-exposed females	Diet	F (2, 30) = 16.48	P < 0.001
	Time	F (3.91, 117.40) = 920.40	P < 0.001
	Diet x Time	F (34, 510) = 8.82	P < 0.001
M) Body weight metformin-treated females	Diet	F (2, 36) = 6.99	P = 0.003
	Time	F (3.15, 113.3) = 471.40	P < 0.001
	Diet x Time	F (34, 612) = 5.42	P < 0.001
N) Body weight P16 females	Diet	F (2, 160) = 11.40	P < 0.001
	Treatment	F (2, 160) = 30.10	P < 0.001
	Diet x Treatment	F (4, 160) = 8.71	P < 0.001
O) Body weight change females	Diet	F (2, 157) = 5.74	P = 0.004
	Treatment	F (2, 157) = 37.50	P < 0.001
	Diet x Treatment	F (4, 157) = 6.05	P < 0.001
P) Glycemia P16 females	Diet	F (2, 76) = 3.86	P = 0.025
	Metformin	F (1, 76) = 3.50	P = 0.065
	Diet x Metformin	F (2, 76) = 1.93	P = 0.152
Q) Insulin levels P16 females	Diet	F (2, 28) = 3.96	P = 0.031
	Metformin	F (1, 28) = 0.06	P = 0.812
	Diet x Metformin	F (2, 28) = 0.36	P = 0.702
R) Leptin levels P16 females	Diet	F (2, 28) = 9.24	P < 0.001
	Metformin	F (1, 28) = 0.04	P = 0.838
	Diet x Metformin	F (2, 28) = 0.69	P = 0.511
S) Ghrelin levels P16 females	Diet	F (2, 31) = 0.41	P = 0.666
	Metformin	F (1, 31) = 9.98	P = 0.004
	Diet x Metformin	F (2, 31) = 0.39	P = 0.682
T) GDF15 levels P16 females	Diet	F (2, 26) = 15.49	P < 0.001
	Metformin	F (1, 26) = 0.21	P = 0.650
	Diet x Metformin	F (2, 26) = 1.23	P = 0.310

Conversely, the opposite trend was observed from P19 onwards with an accelerated increase in body weight in all the HFD-fed groups, regardless of treatment exposure. This was seen in the vehicle group, where both male and female offspring from CD/HFD and HFD/HFD groups surpass the CD/CD offspring from P20 to P21 (Figure 2A,K; $p < 0.001$). This was also seen in the insulin-exposed male offspring, where the HFD/HFD offspring significantly surpass the CD/CD offspring from P20 to P21 (Figure 2B; $p < 0.01$).

We next focused on the analysis of offspring body weight at P16. At this time-point the effects observed in the offspring are solely influenced by maternal nutrition and anti-diabetic treatment exposure, since from P16 onwards, pups are able to free-feed by themselves

[57]. Analysis of male offspring weight at P16 (Figure 2D) revealed a significant interaction between maternal diet and treatment exposure, suggesting a differential response to anti-diabetic treatment dependent on the maternal metabolic state. Compared to vehicle, early metformin treatment significantly reduced body weight in both CD/CD and HFD/HFD male offspring ($p < 0.001$), whereas this effect was not evident in the CD/HFD males. Maternal insulin exposure significantly reduced body weight in male offspring from HFD/HFD mothers ($p < 0.01$) but promoted growth in CD/HFD male offspring ($p < 0.05$). Similar findings were observed in terms of body weight gain (Figure 2E), where metformin exposure reduced weight gain in both CD/CD and HFD/HFD male offspring ($p < 0.001$), but not in CD/HFD male offspring. An increased weight gain in the CD/HFD/INS compared to CD/HFD/MET ($p < 0.01$) was also observed in males.

Similar to males, P16 females (Figure 2N) displayed a reduction in body weight when exposed to metformin during lactation compared to vehicle group in both CD/CD and HFD/HFD groups ($p < 0.001$), but not in CD/HFD offspring. Insulin exposure had an opposite effect dependent on the maternal metabolic state, it promoted body weight gain in the CD/HFD female offspring ($p < 0.05$), but reduced body weight in females born to HFD/HFD mothers ($p < 0.01$). Similar to males, female offspring born from CD/CD and HFD/HFD dams (Figure 2O) exposed to metformin displayed reduced body weight gain from P4 to P16. Insulin exposure also had this effect on HFD/HFD female offspring ($p < 0.001$), but it increased body weight gain in CD/HFD female offspring in comparison to metformin treatment ($p < 0.001$).

Further analysis of the blood glucose levels in P16 males revealed a significant effect of metformin exposure on reducing glycemia (Figure 2F). In females, a significant effect of maternal diet exposure was observed (Figure 2P), with a significant increase of blood glucose levels in CD/HFD/MET offspring compared to CD/CD/MET ($p < 0.05$). This indicates that lactational metformin exposure reduces glycemia in male offspring, but is not able to normalize the HFD-induced hyperglycemia in female offspring. We next assessed the levels of circulating metabolic hormones relevant for the regulation of whole-body energy homeostasis in the offspring. Plasma insulin levels were significantly increased by maternal HFD exposure in both male and female P16 offspring (Figure 2G,Q) as well as circulating leptin levels, which were significantly increased in male offspring from obese mothers (HFD/HFD) compared to control group ($p < 0.01$; Figure 2H) and in both CD/HFD and HFD/HFD metformin-treated female offspring ($p < 0.05$ and $p < 0.01$, respectively; Figure 2R). However, no significant effect of metformin on normalizing the maternal HFD-induced hyperinsulinemia and hyperleptinemia was observed. Interestingly, a significant effect of metformin on reducing total ghrelin plasma levels was found in both male and female offspring, independently of maternal diet exposure (Figure 2I,S). In addition, we measured GDF15 levels in the offspring's plasma, as it plays a role in postnatal growth, cardiometabolic health and adiposity [58]. Circulating GDF15 levels were not significantly affected by maternal HFD or metformin exposure in male offspring (Figure 2J), but they were significantly higher in female offspring from both CD/HFD and HFD/HFD mothers, regardless of metformin treatment (Figure 2T).

Overall, early exposure to anti-diabetic drugs compromises offspring growth, except in offspring from mothers fed with HFD exclusively during the lactation period. In this case, maternal insulin exposure promoted postnatal weight gain but metformin-treated offspring did not differ from vehicle-treated offspring. In addition, early metformin exposure did not counteract the metabolic impairments induced by maternal overnutrition in the offspring.

3.4. Effects of anti-diabetic treatment on hypothalamic neurocircuits are dependent on the maternal metabolic state

To determine the effects on whole animal physiology mediated by brain specific changes, we next focused on the effect of the treatment groups described on the development and function within the hypothalamus, the energy regulating center of the brain. It is known that in neuronal physiology, changes in AMPK signaling can affect axonal outgrowth [35], potentially via increased exposure to circulating factors from the mother crossing into the hypothalamus. Additionally, alterations in AMPK signaling specifically in POMC and AgRP neurons is known to affect metabolic health in animal models [43]. Further, maternal overnutrition can specifically affect the development of AgRP and POMC neuronal projections in the hypothalamus resulting in changes to metabolism [41,42]. Thus, we next explored the effects of maternal overnutrition and anti-diabetic drugs exposure specifically on AgRP and POMC intra-hypothalamic projections in P16 and P21 male and female offspring.

Our results show an effect of anti-diabetic treatment exposure on AgRP neuronal projections in the neuroendocrine or anterior portion of the paraventricular nucleus of the hypothalamus (PVHant) in P16 male offspring (Figure 3A; Table 5), indicating a reduction of AgRP innervation due to insulin and metformin treatments. Whereas no effect was observed in P16 females (Figure 3B). Furthermore, a significant interaction between maternal diet and treatment exposure was seen to affect α-MSH neuronal projections in the PVHant of P16 males (Figure 3C), suggesting that insulin and metformin reduce α-MSH innervation in offspring of control dams, but rescue α-MSH impairments in offspring from obese dams. No differences were observed regarding α-MSH fiber density in P16 females (Figure 3D).

No significant effects of maternal diet or treatment exposure on the density of AgRP-containing fibers onto the pre-autonomic or posterior portion of the PVH (PVHpost) were seen in P16 offspring (Supplementary Fig. 3A, B; Supplementary Table 4), although female offspring from obese mothers (HFD/HFD) seemed to be more affected than those exposed to HFD during lactation (CD/HFD). No changes were observed on α-MSH innervation of the PVHpost in either males or females by P16 (Supplementary Figs. 3C and D).

AgRP fiber density in the PVHant was significantly affected by maternal diet ($p < 0.05$) in P21 male offspring (Figure 4A; Table 6). No significant effects of maternal diet or treatment exposure were observed in the PVHant of P21 females (Figure 4B), although a 34% reduction in AgRP innervation in the offspring from lactational HFD was observed. α-MSH fiber density in the PVHant was not altered in either males or females at weaning (Figure 4C,D). Notwithstanding, a potential effect for maternal insulin treatment on promoting axonal fiber densities was observed in female offspring from obese mothers.

In the PVHpost of P21 male offspring, lactational HFD reduced AgRP fiber density by 44% (Supplementary Fig. 4A; Supplementary Table 5), and this reduction was not rescued by anti-diabetic treatment exposure, although insulin seemed to promote AgRP innervation in male offspring from obese mothers. P21 females exposed to HFD during lactation showed a reduction of 30% of AgRP fiber density in the PVHpost, but no change in those born to obese mothers was observed. In this case, a significant *diet* $\times$ *treatment* interaction ($p < 0.05$) was observed, indicating a differential effect of anti-diabetic treatments dependent on the maternal metabolic state. Insulin and metformin treatment do seem to affect negatively AgRP fiber density in the control group while they seem to recover AgRP innervation impairments induced by maternal HFD exposure (Supplementary Fig. 4B, Supplementary Table 5). No overall changes were observed in α-MSH

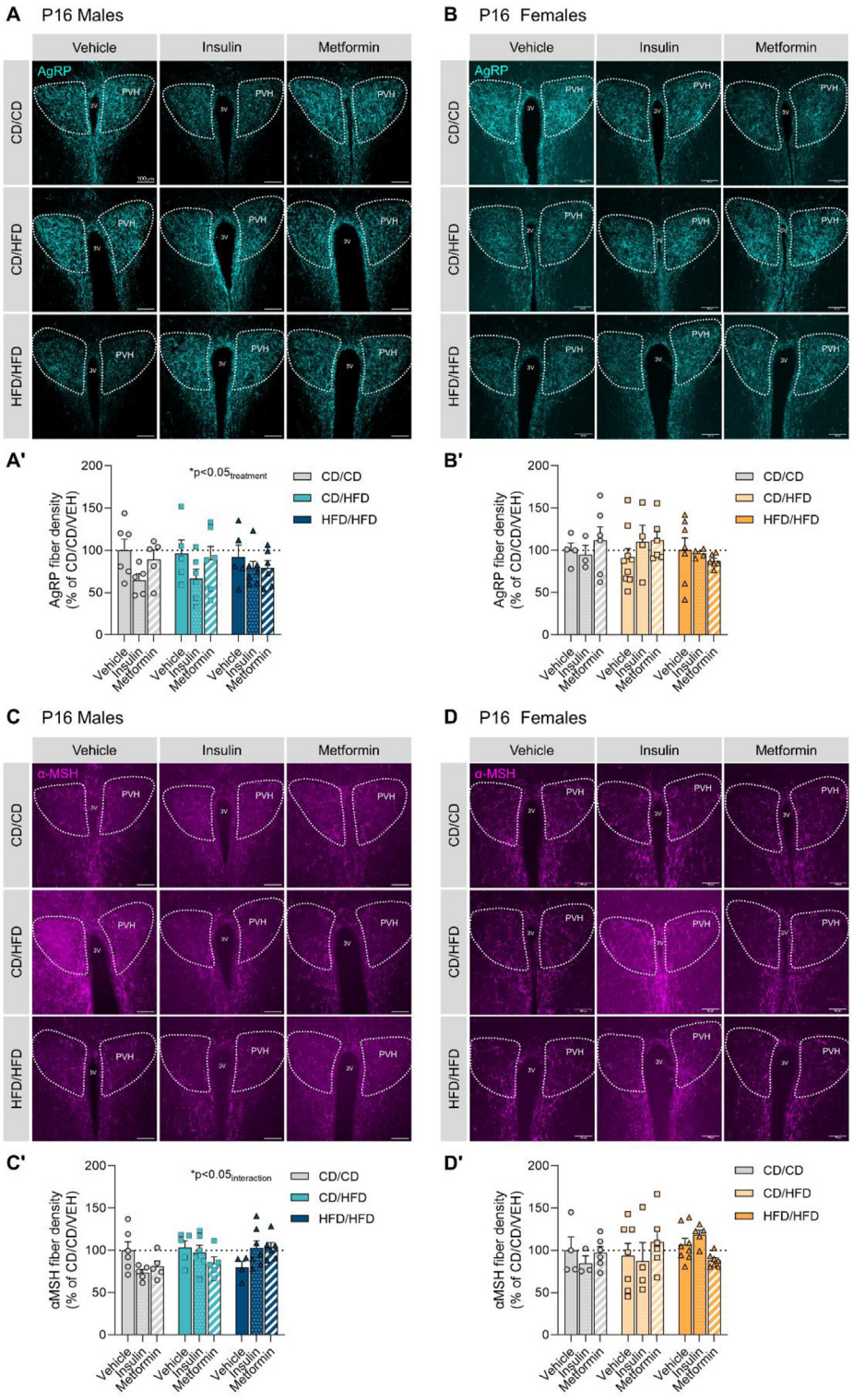

Figure 3: Effects of maternal overnutrition and anti-diabetic treatments on AgRP and α-MSH fiber density in the anterior portion of the paraventricular nucleus of the hypothalamus (PVHant) in P16 offspring. (A, A′) Representative images of AgRP projections and their quantification in the anterior paraventricular nucleus of the hypothalamus (PVH) of P16 male offspring. (B, B′) Representative images of AgRP projections and their quantification in the anterior paraventricular nucleus of the hypothalamus (PVH) of P16 female offspring. (C, C′) Representative images of α-MSH projections and their quantification in the anterior paraventricular nucleus of the hypothalamus (PVH) of P16 male offspring. (D, D′) Representative images of α-MSH projections and their quantification in the anterior paraventricular nucleus of the hypothalamus (PVH) of P16 female offspring. Data are presented as mean ± SEM with single data points. Statistical analyses were performed using two-way ANOVA. Scale bar is 100 μm. 3V: third ventricle; PVH: paraventricular nucleus of the hypothalamus; CD/CD: gestational and lactational control diet-exposed; CD/HFD: gestational control diet and lactational high-fat diet-exposed; HFD/HFD: gestational and lactational high-fat diet-exposed.

Table 5 — Two-way ANOVA results for Figure 3.

Panel	Source of variation	F (DFn, DFd)	P value
A) AgRP fiber density in PVHant on P16 males	Diet	F (2, 42) = 0.01	P = 0.992
	Treatment	F (2, 42) = 3.64	P = 0.035
	Diet x Treatment	F (4, 42) = 0.40	P = 0.805
B) AgRP fiber density in PVHant on P16 females	Diet	F (2, 40) = 0.46	P = 0.635
	Treatment	F (2, 40) = 0.21	P = 0.808
	Diet x Treatment	F (4, 40) = 0.76	P = 0.558
C) α-MSH fiber density in PVHant on P16 males	Diet	F (2, 40) = 1.68	P = 0.199
	Treatment	F (2, 40) = 0.25	P = 0.779
	Diet x Treatment	F (4, 40) = 3.13	P = 0.025
D) α-MSH fiber density in PVHant on P16 females	Diet	F (2, 41) = 0.66	P = 0.521
	Treatment	F (2, 41) = 0.05	P = 0.952
	Diet x Treatment	F (4, 41) = 1.64	P = 0.182

fiber density in the PVHpost of P21 males (Supplementary Fig. 4C), whereas a significant interaction of *diet* and *treatment* ($p < 0.001$) was observed in females (Supplementary Fig. 4D; Supplementary Table 5). This provides further evidence that anti-diabetic treatment alters α-MSH fiber density in a maternal metabolic state dependent manner.

Collectively, our results indicate that the most detrimental effects of maternal HFD feeding during lactation on hypothalamic AgRP neuronal fiber densities can be observed in females at P21. Further, insulin treatment in dams fed a HFD prior to mating, and during pregnancy and lactation, seems to promote axonal outgrowth of both AgRP and POMC neurons in female offspring by P21. Although maternal insulin exposure seems to reduce neuronal innervation in control group offspring. Metformin exposure does not significantly alter axonal outgrowth, but slightly increases AgRP and α-MSH innervation in P21 female offspring born to HFD-fed dams exclusively during the lactation period.

3.5. Metformin exposure does not affect AgRP or POMC neuronal number in the arcuate nucleus

Metformin has been shown to have an age-dependent effect on neurogenesis resulting in a significant increase of the neural stem cell pool, specifically with maximal effect upon exposure during the early postnatal phase [59]. To determine if neurogenesis in hypothalamic neuronal populations responsible for homeostatic control is affected by the early exposure, AgRP- and POMC-Cre male animals were crossed to TdTomato-floxed females to generate offspring with labeled neuronal populations. In two subregions of the ARH, AgRP neuronal cell number was analysed (Figure 5A and Supplementary Fig. 5A) with no significant effect of dietary or pharmacological treatment (Table 7; Supplementary Table 6). POMC neuronal populations were also imaged and quantified (Figure 5B and Supplementary Fig. 5B), but no overall effect of early metformin exposure was uncovered (Table 7). In the most rostral ARH, a slight but significant decrease in neuronal number, due to maternal HFD exposure was seen, which was not restored by metformin (Supplementary Fig. 5B, B'; Supplementary Table 6). This suggests that early postnatal metformin exposure does not result in changes to POMC or AgRP cell number in the ARH.

3.6. Early metformin exposure induces sex-specific changes to hypothalamic AMPK signaling

To determine the lasting impact of metformin exposure on known intracellular signaling pathways, protein levels of AMPK signaling components were assayed in the hypothalamus of 16-day-old male and female mice with metformin treatment from P4—P15. Samples were collected 16 h after the last metformin exposure, to ensure long-lasting effects of metformin treatment and not acute pathway activation. Analysis of AMPK activation revealed an overall significant effect of maternal diet exposure on the expression of AMPK in both male and female offspring (Figures 6A and 7A; Table 8, Table 9). However, levels of phosphorylated-AMPK were significantly altered by diet in males (Figure 6B), but only moderately affected by metformin exposure ($p_{metformin} = 0.062$) ultimately resulting in no overall differences to AMPK activation (Figure 6C). Conversely in females, no change in p-AMPK levels was uncovered (Figure 7B). When assessing overall AMPK activation as a result, a significant effect of maternal diet was uncovered (Figure 7C). Therefore, exposure to altered maternal metabolic states in early development results in subtle but distinct changes to AMPK signaling pathways with unique effects between sexes.

We next explored the protein expression levels of liver kinase B1 (LKB1), as it is the main upstream kinase in the AMPK pathway known to be involved in cell polarity regulation [60,61] and for being a main target of metformin's action [62]. No significant changes in the protein levels of LKB1 or its phosphorylated form were found in P16 male offspring hypothalamus (Figure 6D,E and F; Table 8). Notwithstanding, in P16 females, metformin significantly increased the levels of phosphorylated LKB1 (Figure 7E), which indicates a significant induction of LKB1 activation by metformin (Figure 7F), as no changes were observed in total LKB1 levels (Figure 7D; Table 9).

AMPK has multiple downstream targets, one of which is the mammalian target of rapamycin (mTOR), which stimulates protein synthesis. AMPK inhibits mTOR complex 1 (mTORC1) both directly and indirectly [63], and metformin has been shown to inhibit mTORC1 via AMPK [64]. In an attempt to elucidate the consequences of maternal overnutrition and early metformin exposure on AMPK signaling downstream effectors, we assessed mTOR protein expression. In P16 males, a two-way ANOVA analysis revealed a significant interaction between maternal diet and metformin treatment in total mTOR levels ($p_{interaction}<0.05$), although there was no significant effect of individual factors (Figure 6G, Table 8). This indicates that mTOR expression might change differentially to the combination of both maternal diet and metformin exposure. Maternal diet had a significant effect on the phosphorylated-mTOR levels, potentially driven by the increase observed in the HFD/HFD group (Figure 6H), and metformin treatment seemed to induce mTOR activation ($p_{metformin} = 0.059$) in the hypothalamus of male offspring (Figure 6I). In females, no significant changes of total mTOR levels (Figure 7G), phosphorylated-mTOR levels (Figure 7H) or p-mTOR/mTOR ratio were observed (Figure 7I; Table 9). Furthermore, activation of AMPK inhibits fatty acid *de novo* synthesis via phosphorylation and inactivation of acetyl-CoA carboxylase (ACC), and metformin has indeed been shown to reduce ACC activity [65]. Thus, we also assessed ACC phosphorylation levels in the hypothalamus of P16 offspring. No changes in total ACC levels were observed either in males (Figure 6J) or females (Figure 7J), but increased ACC phosphorylation due to metformin treatment was observed in males (Figure 6K; Table 8), although not in females (Figure 7K; Table 9). However, no significant effects of metformin nor maternal diet were found on the p-ACC/ACC ratio in males (Figure 6L) or females (Figure 7L).

Overall, despite increased phosphorylation of LKB1 in the hypothalamus of P16 female offspring by early metformin treatment, there were no further significant changes to the AMPK signaling cascade. In males, although no changes in LKB1 or AMPK phosphorylation, due to metformin exposure, were detected, slight trends toward increased mTOR activation and significant ACC phosphorylation were observed. Maternal overnutrition was found to decrease levels of p-AMPK while increasing p-mTOR levels in males; whereas in females, maternal

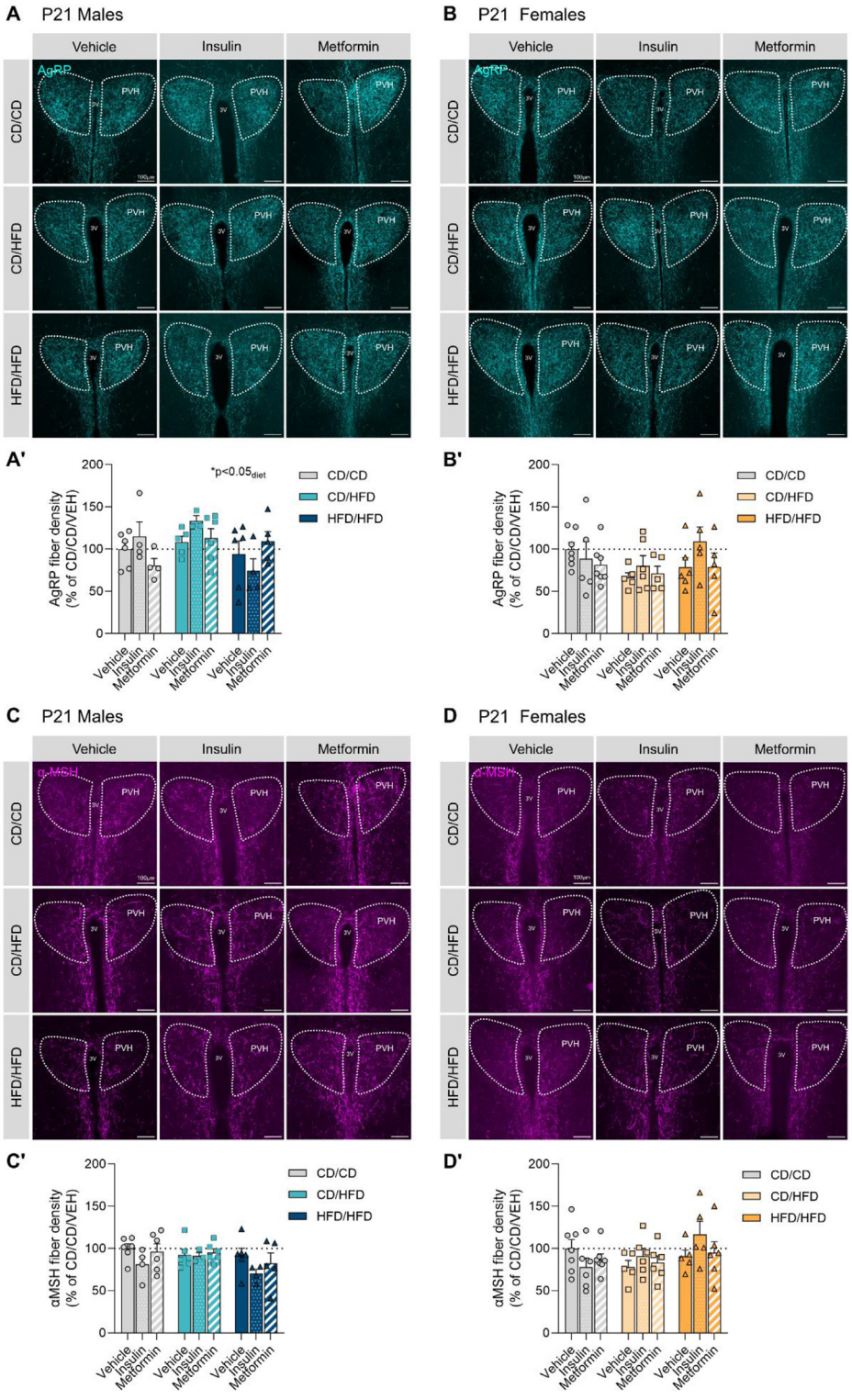

Figure 4: Effects of maternal overnutrition and anti-diabetic treatments on AgRP and α-MSH fiber density in the anterior portion of the paraventricular nucleus of the hypothalamus (PVHant) in P21 offspring. (A, A′) Representative images of AgRP projections and their quantification in the anterior paraventricular nucleus of the hypothalamus (PVH) of P21 male offspring. (B, B′) Representative images of AgRP projections and their quantification in the anterior paraventricular nucleus of the hypothalamus (PVH) of P21 female offspring. (C, C′) Representative images of α-MSH projections and their quantification in the anterior paraventricular nucleus of the hypothalamus (PVH) of P21 male offspring. (D, D′) Representative images of α-MSH projections and their quantification in the anterior paraventricular nucleus of the hypothalamus (PVH) of P21 female offspring. Data are presented as mean ± SEM with single data points. Statistical analyses were performed using two-way ANOVA. Scale bar is 100 μm. 3V: third ventricle; PVH: paraventricular nucleus of the hypothalamus; CD/CD: gestational and lactational control diet-exposed; CD/HFD: gestational control diet and lactational high-fat diet-exposed; HFD/HFD: gestational and lactational high-fat diet-exposed.

Table 6 — Two-way ANOVA results for Figure 4.

Panel	Source of variation	F (DFn, DFd)	P value
A) AgRP fiber density in PVHant on P21 males	Diet	F (2, 34) = 3.42	P = 0.044
	Treatment	F (2, 34) = 0.25	P = 0.777
	Diet x Treatment	F (4, 34) = 2.17	P = 0.093
B) AgRP fiber density in PVHant on P21 females	Diet	F (2, 42) = 1.76	P = 0.185
	Treatment	F (2, 42) = 1.15	P = 0.325
	Diet x Treatment	F (4, 42) = 0.81	P = 0.529
C) α-MSH fiber density in PVHant on P21 males	Diet	F (2, 37) = 1.90	P = 0.164
	Treatment	F (2, 37) = 2.02	P = 0.147
	Diet x Treatment	F (4, 37) = 0.44	P = 0.779
D) α-MSH fiber density in PVHant on P21 females	Diet	F (2, 44) = 1.94	P = 0.155
	Treatment	F (2, 44) = 0.36	P = 0.697
	Diet x Treatment	F (4, 44) = 1.50	P = 0.220

overnutrition promoted activation of both AMPK and its upstream kinase LKB1.

Hence, sex-, diet- and metformin-specific effects were found in various components of the AMPK signaling cascade in the developing hypothalamus (Figure 8), which ultimately lead to cumulative changes that may alter hypothalamic function.

3.7. Sex dependent changes in transporters responsible for metformin access to the brain

Given the sex specific results we have shown to this point, we next explored if metformin access to the brain during development may be different between sexes as a putative explanation to the sex differences noted thus far. In order to reach the brain to elicit changes in projections and hypothalamic signaling, metformin must gain access to this privileged tissue. Is it known that metformin is a substrate of polyspecific organic cation transporters (Octs) in peripheral organs, such as the liver and kidney, where Octs are the major determinants for metformin absorption and clearance. Octs, including *Oct1* and *Oct3*, are also expressed in the brain [66], where they contribute to the absorption and clearance of various physiological compounds. Recently, Sharma et al. [67] demonstrated that metformin can cross the blood—brain barrier (BBB) using *Oct1* for its transport.

To determine the potential for exposure of the neonatal mouse brain to metformin during the early postnatal period, we assessed the gene expression levels of transporters responsible for metformin uptake and efflux [67,68] in the developing hypothalamus. Expression was assessed at different time-points during the time window in which the pharmacological interventions took place in our study. Expression at 8 weeks of age was also assessed (Figure 9; Table 10). Robust changes in organic cation transporter 1 (*Oct1)* mRNA expression were seen from P6 and throughout the lactation period in both males and females. *Oct1* expression in males was reduced from P6 to P9 ($p < 0.05$), although its expression was restored by P21 ($p < 0.05$) and maintained until adulthood ($p < 0.001$) (Figure 9A). By contrast, *Oct1* expression in females was reduced from P6 to P9 ($p < 0.001$) and was kept low throughout development (Figure 9D). Interestingly, expression of the organic cation transporter 3 (*Oct3*) increased across the lactational period in females, with a robust upregulation from P6 to P9 ($p < 0.001$), which was maintained until P16. At P21, *Oct3* expression was reduced compared to P9 levels ($p < 0.05$) (Figure 9E). In males, a different expression profile was noted, *Oct3* decreased across this period with a significant reduction being reached by P21 ($p < 0.01$) (Figure 9B). In adulthood, females displayed a 6-fold increase in *Oct3* expression, whereas in males, this response was not evident. Expression of multidrug and toxic extrusion 1 (*Mate1*), which plays a role in metformin's clearance, was also detected in the developing hypothalamus of both males and females (Figure 9C,F), although a dynamic upregulation of its expression across development was only observed in females; specifically, from P6 to P11 ($p < 0.01$).

We demonstrated a dynamic gene expression of *Oct1*, *Oct3* and *Mate1*, transporters responsible for metformin cell permeability, during the early postnatal phase in the hypothalamus. Sex-specific patterns of expression were observed, which could account for differences in response to metformin between sexes.

4. DISCUSSION

With the increasing occurrence of both pre-pregnancy obesity and GDM, as well as their co-occurrence, pharmacological interventions in early development are becoming more common. However, understanding the potential long-term consequences of early exposure is still needed. While many interventions show promise in the immediate sense, through improved birth outcomes, there is evidence emerging that anti-diabetic treatments in early development may manifest into metabolic changes later in life [17,18]. Here we show that dependent on maternal metabolic state, a variety of metabolic outcomes can occur after early metformin exposure in mice.

4.1. Anti-diabetic treatment effects in mothers vary due to maternal metabolic state

In our study, we utilized a model of two different maternal metabolic conditions during pregnancy and lactation periods by exposing the dams to HFD during different periods of time and tracking the physiological changes in response to the dietary intervention. Interestingly, only the lactational HFD model showed a dramatic weight gain reminiscent of GWG in humans, whereas the pre-pregnancy HFD-exposed group showed similar rates of weight gain as the control diet-fed group throughout pregnancy and a maintenance of body weight, albeit significantly higher than the control group, during the lactation phase. While many studies of maternal obesity in animal models rely on the pre-pregnancy exposure to HFD, we explicitly sought out a way to mimic gestational weight gain, or this increase in body weight in the period equivalent to the third trimester of brain development in humans [50]. We were successful in this model to drive consistent weight gain in the lactation period, not seen in the other two dietary groups and could monitor how this metabolic environment, i.e. weight gain above normal levels, contributes to offspring metabolic outcomes. Given that more than 50% of all pregnancies show excessive gestational weight gain regardless of pre-pregnancy body weight, a model for understanding how gestational weight gain alone contributes to alterations in brain development is relevant for continued analysis of neuronal circuits [69]. Accordingly, lactational HFD exposure alone induced more metabolic abnormalities in offspring mice than maternal HFD throughout gestation and lactation [70] and in humans, the maternal metabolic profile has been shown to have a differential impact on child neurodevelopment [71].

Interestingly, our results show an increase in food intake in the metformin-treated mothers exposed to HFD during lactation only, which may explain the offspring weight loss prevention in this group. However, this effect of metformin is unexpected, as metformin is known to produce anorectic effects by modulating the expression of hypothalamic neuropeptides and leptin receptor [72] [—] [74] and to reduce feelings of hunger in humans [75]. Nevertheless, the excessive food consumption in that group of dams did not lead to increased maternal weight gain or increased blood glucose levels. This may also indicate an alternative effect of metformin in pregnancy on food intake and could warrant additional human studies in this regard.

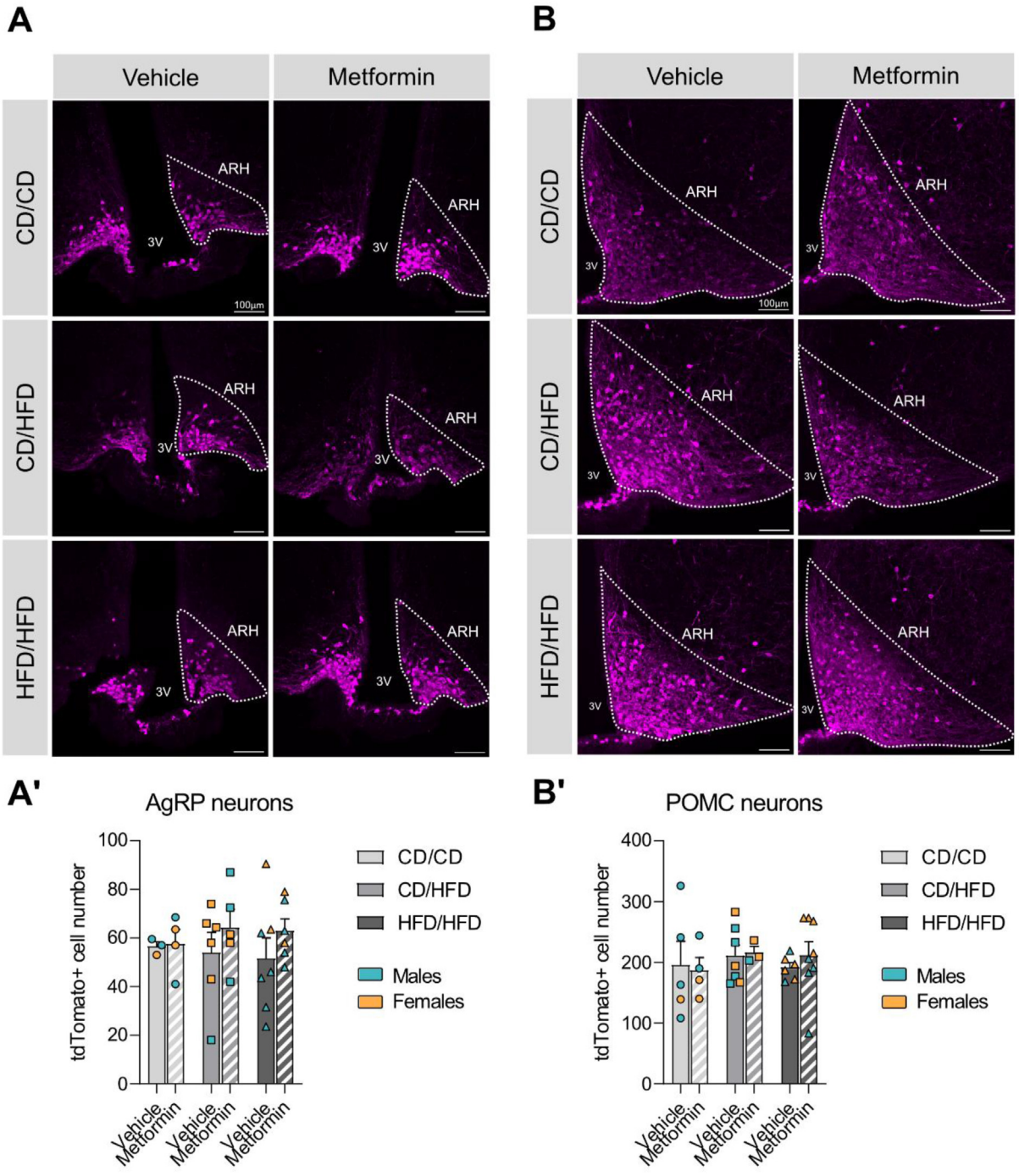

Figure 5: Metformin does not have an impact on the cell number of the two main arcuate neuronal populations. (A, A′) Representative images of TdTomato-labelled AgRP neurons and their quantification in the mid-portion of the ARH. (B, B′) Representative images of TdTomato-labelled POMC neurons and their quantification in the mid-portion of the ARH. Data are presented as mean ± SEM with single data points. Blue dots represent males and orange dots represent females. Statistical analyses were performed using two-way ANOVA. Scale bar is 100 µm. 3V: third ventricle; ARH: arcuate nucleus of the hypothalamus; CD/CD: gestational and lactational control diet-exposed; CD/HFD: gestational control diet and lactational high-fat diet-exposed; HFD/HFD: gestational and lactational high-fat diet-exposed.

In our study, both models of maternal overnutrition led to hyperglycemia by the end of the lactation period, which was not rescued by the anti-diabetic treatments. However, since blood samples were taken on the day following the last treatment administration (approximately 16 h after the last exposure), it is likely that the acute glucose lowering effect of these drugs is no longer present. It is known that metformin has a plasmatic half-life of 2–6 h [76], and even though new basal insulin analogs have a longer half-life, the peak of glucose-lowering action occurs at 4–5 h [77]. However, it should be noted that in humans studies which assessed glucose levels at 36 weeks of gestation, metformin had no glucose-lowering effects [78]. Still, an effect of metformin on both insulin and leptin circulating levels can be observed in our study, with metformin being able to normalize the HFD-induced hyperinsulinemia and hyperleptinemia in the mothers. In

Table 7 — Two-way ANOVA results for Figure 5.

Panel	Source of variation	F (DFn, DFd)	P value
A) AgRP neuronal cell number in mid ARH	Diet	F (2, 25) = 0.04	P = 0.958
	Metformin	F (1, 25) = 1.38	P = 0.252
	Diet x Metformin	F (2, 25) = 0.22	P = 0.802
B) POMC neuronal cell number in mid ARH	Diet	F (2, 27) = 0.37	P = 0.697
	Metformin	F (1, 27) = 0.07	P = 0.789
	Diet x Metformin	F (2, 27) = 0.20	P = 0.823

agreement with this, metformin has been shown to reduce insulin levels in both lean and obese patients after 3 months of treatment [79]. Both insulin and leptin serum levels were also reduced after a 16-week metformin treatment in a dose-dependent manner in mice [80] and insulin levels were also reduced in dams exposed to metformin during the lactation period [32]. In addition, metformin treatment led to increased circulating GDF15 levels in the mothers. Consistent with our findings, metformin is known to increase circulating GDF15 levels [81]. The induction of GDF15 levels by metformin was more evident in the

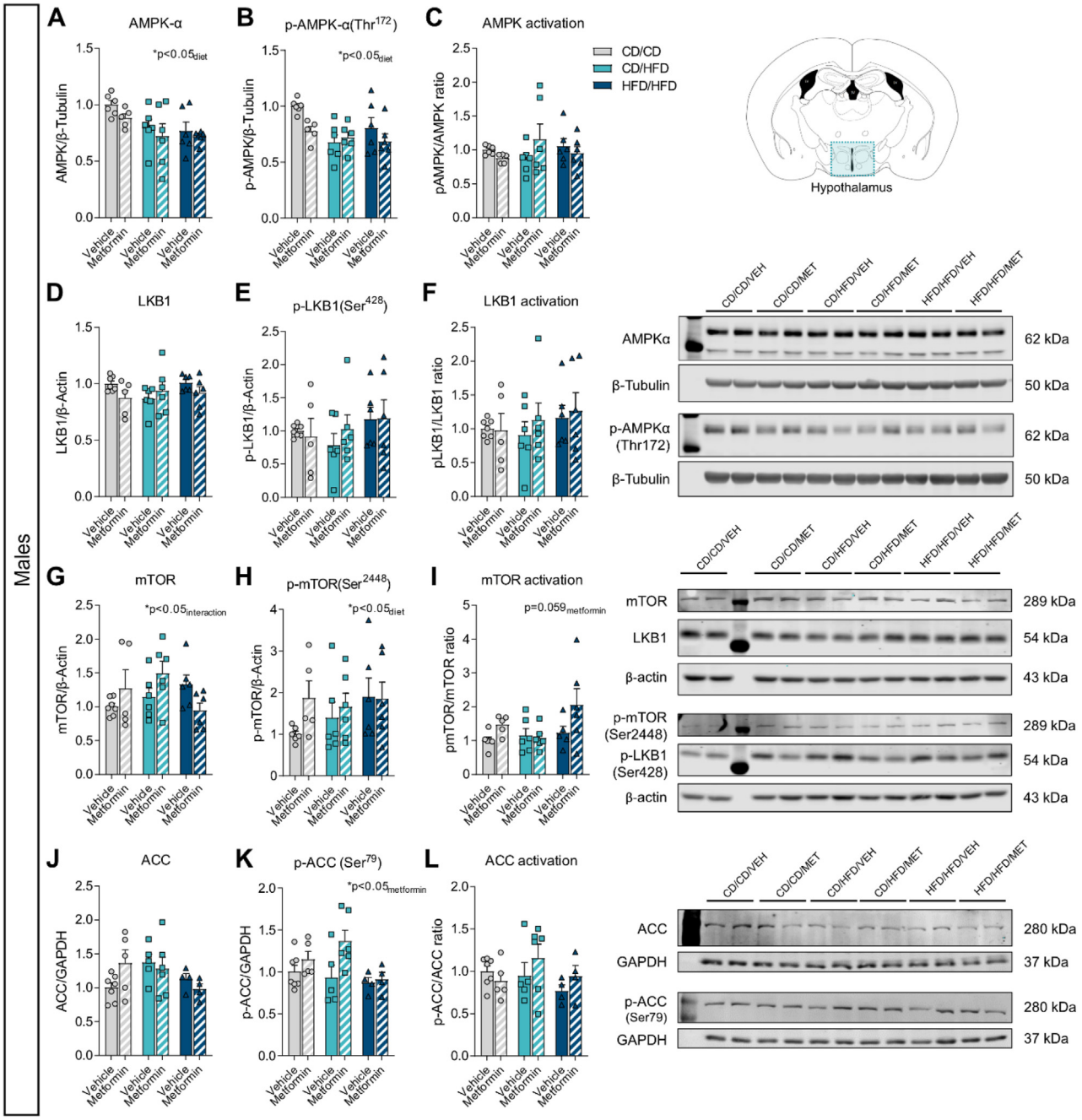

Figure 6: Comprehensive analysis of the classical signaling pathway of metformin's mechanism of action in the hypothalamus of P16 male offspring. Relative protein expression of (A) total AMPKα levels, (B) phosphorylated-AMPKα(Thr^{172}) levels and (C) AMPK activation ratio; (D) total LKB1 levels, (E) phosphorylated-LKB1(Ser^{428}) levels and (F) LKB1 activation ratio; (G) total mTOR levels, (H) phosphorylated-mTOR(Ser^{2448}) levels and (I) mTOR activation ratio; and (J) total ACC levels, (K) phosphorylated-ACC(Ser^{79}) levels and (L) ACC activation ratio (n = 6/group). Data are presented as mean ± SEM with single data points. Statistical analyses were performed using two-way ANOVA. CD/CD: gestational and lactational control diet-exposed; CD/HFD: gestational control diet and lactational high-fat diet-exposed; HFD/HFD: gestational and lactational high-fat diet-exposed.

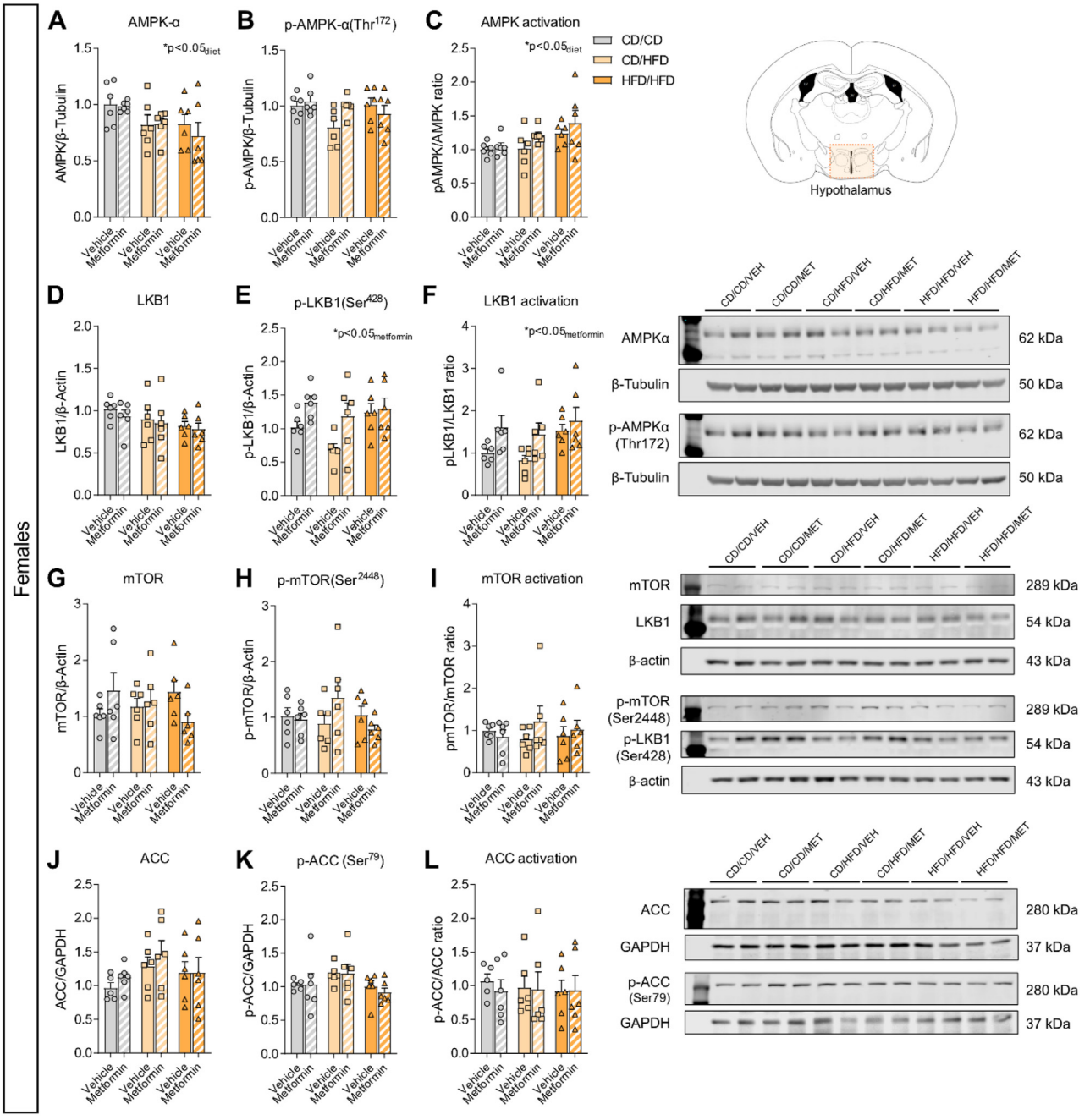

Figure 7: Comprehensive analysis of the classical signaling pathway of metformin's mechanism of action in the hypothalamus of P16 female offspring. Relative protein expression of (A) total AMPKα levels, (B) phosphorylated-AMPKα(Thr^{172}) levels and (C) AMPK activation ratio; (D) total LKB1 levels, (E) phosphorylated-LKB1(Ser^{428}) levels and (F) LKB1 activation ratio; (G) total mTOR levels, (H) phosphorylated-mTOR(Ser^{2448}) levels and (I) mTOR activation ratio; and (J) total ACC levels, (K) phosphorylated-ACC(Ser^{79}) levels and (L) ACC activation ratio (n = 6/group). Data are presented as mean ± SEM with single data points. Statistical analyses were performed using two-way ANOVA. CD/CD: gestational and lactational control diet-exposed; CD/HFD: gestational control diet and lactational high-fat diet-exposed; HFD/HFD: gestational and lactational high-fat diet-exposed.

CD/CD and HFD/HFD groups than in dams exposed to HFD during lactation. This could explain the reduction of food intake observed in the metformin-treated dams in these two groups, as GDF15 has been linked to appetite suppression [82].

Metformin administration through the drinking water (3 mg/ml) in our study led to maternal serum levels from 5 μM to 100 μM, averaging around 40 μM in all groups, regardless of the maternal dietary intervention. These levels are comparable to previous studies in rodents of oral administration of metformin, that report plasma concentrations of 5 μM—180 μM. Moreover, this is similar to circulating levels in humans of 10—40 μM that result from a therapeutic dose of 500—2500 mg/day of metformin [52,83]. Importantly, in our study, similar serum metformin concentrations were reached in all groups of mothers, despite differences in their total amount of water intake. Furthermore, as all pups were given intraperitoneal injections of metformin during the suckling period, they all received the same dose.

Table 8 — Two-way ANOVA results for Figure 6.

Panel	Source of variation	F (DFn, DFd)	P value
A) Total AMPKα levels (males)	Diet	F (2, 29) = 4.82	P = 0.016
	Metformin	F (1, 29) = 2.03	P = 0.165
	Diet x Metformin	F (2, 29) = 0.12	P = 0.890
B) Phosphorylated- AMPKα levels (males)	Diet	F (2, 29) = 4.74	P = 0.017
	Metformin	F (1, 29) = 3.76	P = 0.062
	Diet x Metformin	F (2, 29) = 2.20	P = 0.129
C) pAMPK/AMPK ratio (males)	Diet	F (2, 29) = 0.20	P = 0.816
	Metformin	F (1, 29) = 0.04	P = 0.835
	Diet x Metformin	F (2, 29) = 1.87	P = 0.173
D) Total LKB1 levels (males)	Diet	F (2, 30) = 0.65	P = 0.530
	Metformin	F (1, 30) = 1.21	P = 0.279
	Diet x Metformin	F (2, 30) = 1.89	P = 0.169
E) Phosphorylated-LKB1 levels (males)	Diet	F (2, 30) = 1.07	P = 0.355
	Metformin	F (1, 30) = 0.11	P = 0.740
	Diet x Metformin	F (2, 30) = 0.35	P = 0.710
F) pLKB1/LKB1 ratio (males)	Diet	F (2, 30) = 0.68	P = 0.514
	Metformin	F (1, 30) = 0.34	P = 0.566
	Diet x Metformin	F (2, 30) = 0.17	P = 0.844
G) Total mTOR levels (males)	Diet	F (2, 30) = 0.95	P = 0.396
	Metformin	F (1, 30) = 0.38	P = 0.542
	Diet x Metformin	F (2, 30) = 3.53	P = 0.042
H) Phosphorylated-mTOR levels (males)	Diet	F (2, 29) = 0.84	P = 0.444
	Metformin	F (1, 29) = 1.48	P = 0.233
	Diet x Metformin	F (2, 29) = 0.81	P = 0.456
I) p-mTOR/mTOR levels (males)	Diet	F (2, 28) = 2.37	P = 0.112
	Metformin	F (1, 28) = 3.88	P = 0.059
	Diet x Metformin	F (2, 28) = 1.65	P = 0.209
J) Total ACC levels (males)	Diet	F (2, 25) = 1.89	P = 0.173
	Metformin	F (1, 25) = 0.13	P = 0.724
	Diet x Metformin	F (2, 25) = 2.21	P = 0.131
K) Phosphorylated-ACC levels (males)	Diet	F (2, 25) = 2.56	P = 0.097
	Metformin	F (1, 25) = 5.21	P = 0.031
	Diet x Metformin	F (2, 25) = 1.66	P = 0.211
L) pACC/ACC levels (males)	Diet	F (2, 25) = 1.16	P = 0.331
	Metformin	F (1, 25) = 0.73	P = 0.400
	Diet x Metformin	F (2, 25) = 1.10	P = 0.349

Table 9 — Two-way ANOVA results for Figure 7.

Panel	Source of variation	F (DFn, DFd)	P value
A) Total AMPKα levels (females)	Diet	F (2, 30) = 3.99	P = 0.029
	Metformin	F (1, 30) = 0.34	P = 0.562
	Diet x Metformin	F (2, 30) = 0.26	P = 0.776
B) Phosphorylated- AMPKα levels (females)	Diet	F (2, 30) = 1.99	P = 0.154
	Metformin	F (1, 30) = 1.10	P = 0.302
	Diet x Metformin	F (2, 30) = 2.79	P = 0.077
C) pAMPK/AMPK ratio (females)	Diet	F (2, 30) = 4.42	P = 0.021
	Metformin	F (1, 30) = 2.54	P = 0.122
	Diet x Metformin	F (2, 30) = 0.32	P = 0.727
D) Total LKB1 levels (females)	Diet	F (2, 30) = 2.07	P = 0.144
	Metformin	F (1, 30) = 0.62	P = 0.438
	Diet x Metformin	F (2, 30) = 0.05	P = 0.952
E) Phosphorylated-LKB1 levels (females)	Diet	F (2, 30) = 3.26	P = 0.053
	Metformin	F (1, 30) = 7.52	P = 0.010
	Diet x Metformin	F (2, 30) = 1.36	P = 0.273
F) pLKB1/LKB1 ratio (females)	Diet	F (2, 30) = 2.65	P = 0.087
	Metformin	F (1, 30) = 6.79	P = 0.014
	Diet x Metformin	F (2, 30) = 0.45	P = 0.640
G) Total mTOR levels (females)	Diet	F (2, 30) = 0.07	P = 0.932
	Metformin	F (1, 30) = 0.004	P = 0.950
	Diet x Metformin	F (2, 30) = 2.77	P = 0.079
H) Phosphorylated-mTOR levels (females)	Diet	F (2, 30) = 0.67	P = 0.521
	Metformin	F (1, 30) = 0.12	P = 0.736
	Diet x Metformin	F (2, 30) = 2.06	P = 0.145
I) p-mTOR/mTOR levels (females)	Diet	F (2, 30) = 0.07	P = 0.935
	Metformin	F (1, 30) = 0.65	P = 0.427
	Diet x Metformin	F (2, 30) = 0.83	P = 0.448
J) Total ACC levels (females)	Diet	F (2, 29) = 1.99	P = 0.156
	Metformin	F (1, 29) = 0.71	P = 0.408
	Diet x Metformin	F (2, 29) = 0.17	P = 0.842
K) Phosphorylated-ACC levels (females)	Diet	F (2, 29) = 2.54	P = 0.096
	Metformin	F (1, 29) = 0.08	P = 0.774
	Diet x Metformin	F (2, 29) = 0.13	P = 0.875
L) pACC/ACC levels (females)	Diet	F (2, 29) = 0.06	P = 0.941
	Metformin	F (1, 29) = 0.12	P = 0.735
	Diet x Metformin	F (2, 29) = 0.09	P = 0.914

This is important and clinically relevant as the estimated dose of metformin that can reach the infant through the breast milk is 0.5–0.65% of the mother's weight-adjusted dose [83].

4.2. Overall effects of metformin on offspring physiology

If we further probe the effects uncovered specifically in the offspring, the effects of maternal overnutrition are the primary drivers of physiological difference the benefits of metformin treatment diminish. By tracking the offspring's weight, it can be noted that the untreated offspring exposed to maternal overnutrition, in either model, are smaller across the early postnatal period, although an elevated body weight of the offspring exposed to maternal overnutrition appears in the pre-weaning period (P16–P21) due to the offspring free-feeding HFD, consistent with previous animal studies [84]. Notably, being born small for gestational age has been associated with increased fat mass accumulation in infants [85]. Exposure to anti-diabetic drugs during the suckling period reduced both male and female offspring weight by P16, only the offspring exposed to lactational HFD showed no weight loss with metformin treatment, and they even showed an increased body weight with maternal insulin exposure. Indeed, any exposure to anti-diabetic treatment (insulin or metformin) in the context of maternal GWG resulted in an increased body weight as compared to the control fed or the maternal obese condition. This underscores the necessity of including maternal weight trajectory as a parameter in interventional planning.

Interestingly, human studies of GDM-affected pregnancies show that children exposed to metformin *in utero* are smaller at birth than those whose mothers were treated with insulin [86]. However, metformin-exposed children do become heavier, with higher BMI, in childhood. This result warrants an understanding of the post weaning effects of metformin exposure on growth trajectories and physiology in adulthood.

The assessment of circulating levels of metabolic hormones in P16 offspring revealed a glucose-lowering effect of perinatal metformin exposure in male offspring, with no effect of maternal overnutrition, whereas in females, a hyperglycemic effect of maternal overnutrition was observed, which was not rescued by metformin exposure. This glucose-lowering effect of metformin is well known and may explain the reduced growth trajectory of the offspring treated with metformin. However, previous research showed no effects of metformin exposure during lactation on fed glucose levels in P16 male offspring [32]. In our study, maternal HFD exposure increased the circulating levels of insulin and leptin in both male and female offspring in a dose-dependent manner, as offspring from HFD-fed mothers throughout pregnancy and lactation periods displayed higher levels than offspring from lactational HFD-fed mothers. In line with this, increased serum leptin levels have also been found in offspring from obese dams [87,88], specifically from P9 to P18, reflecting a prolonged neonatal leptin surge, which has been related to long-lasting leptin resistance, fat accumulation and obesity. Although not statistically significant, metformin seems to counteract the maternal HFD-induced increase in insulin levels in male offspring. Previous studies have also shown that maternal metformin exposure reduces plasma insulin levels in the offspring of obese dams at weaning [89]. Furthermore, we observed an effect of early

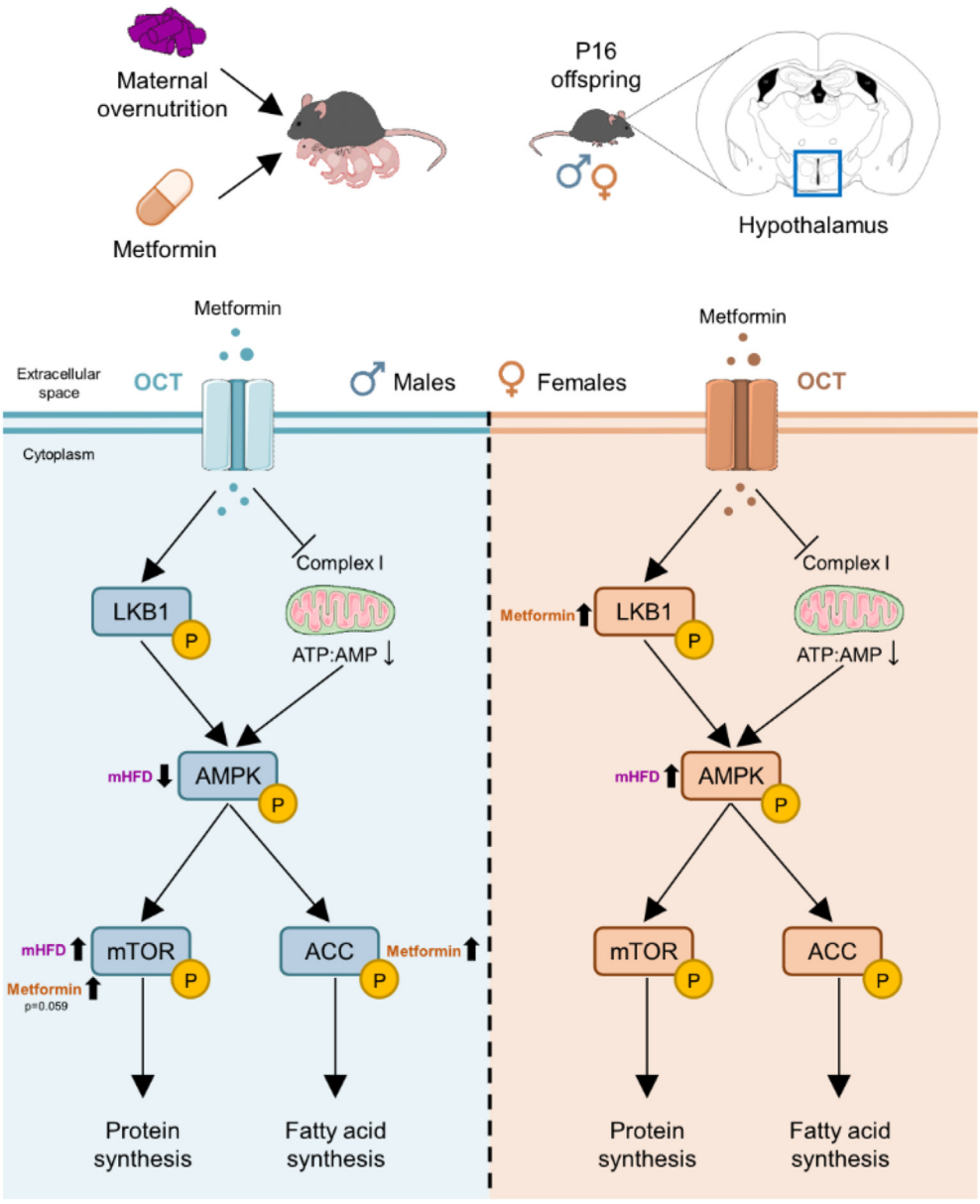

Figure 8: Overview of maternal overnutrition and early metformin exposure effects on the AMPK signaling cascade in the developing hypothalamus of males and females. Maternal overnutrition affected differentially AMPK activation in a sex-specific manner. Early metformin exposure increased phosphorylation of the upstream kinase LKB1 in females, whereas downstream components of AMPK signaling were affected in males. Significant effects of diet exposure or metformin treatment on the phosphorylation of the proteins assessed in the hypothalamus of P16 males (left panel) or P16 females (right panel) are indicated by the black thick arrows. ACC: acetyl-CoA carboxylase; AMPK: AMP-activated protein kinase; LKB1: liver kinase B1; mHFD: maternal high-fat diet; mTORC1: mammalian target of rapamycin complex 1; OCT: organic cation transporter; P: postnatal day; TSC1/2: tuberous sclerosis complex 1/2.

metformin exposure on reducing ghrelin levels in both P16 males and females. Metformin has been shown to inhibit ghrelin release from primary gastric cells [90], which could be related to its mechanism of food intake suppression; however, no alterations in ghrelin levels have been reported in children exposed to metformin *in utero* [91]. In addition, we found elevated GDF15 levels in the offspring born to HFD-fed mothers, especially in females. This could explain the reduction of body weight observed from P4 to P16 in the offspring with maternal overnutrition, at least in the vehicle-treated group. However, early metformin exposure did not significantly alter GDF15 levels in the offspring. As plasma samples were obtained approximately 16 h after the last metformin administration and metformin induction of GDF15 levels is transient, with the highest peak at 4–8 h after metformin administration [81], it is possible that levels were restored to baseline levels when analysed.

4.3. Maternal metformin treatment alters hypothalamic development and AMPK signaling in offspring

It is well established in the metabolic programming field that an intrauterine obesogenic environment alters the hypothalamic neuronal connectivity, as ARH-derived axonal projections onto other intrahypothalamic nuclei develop during the first postnatal weeks in rodents. Critically, disruption of hypothalamic neuronal structure and function in early development increases the susceptibility to develop

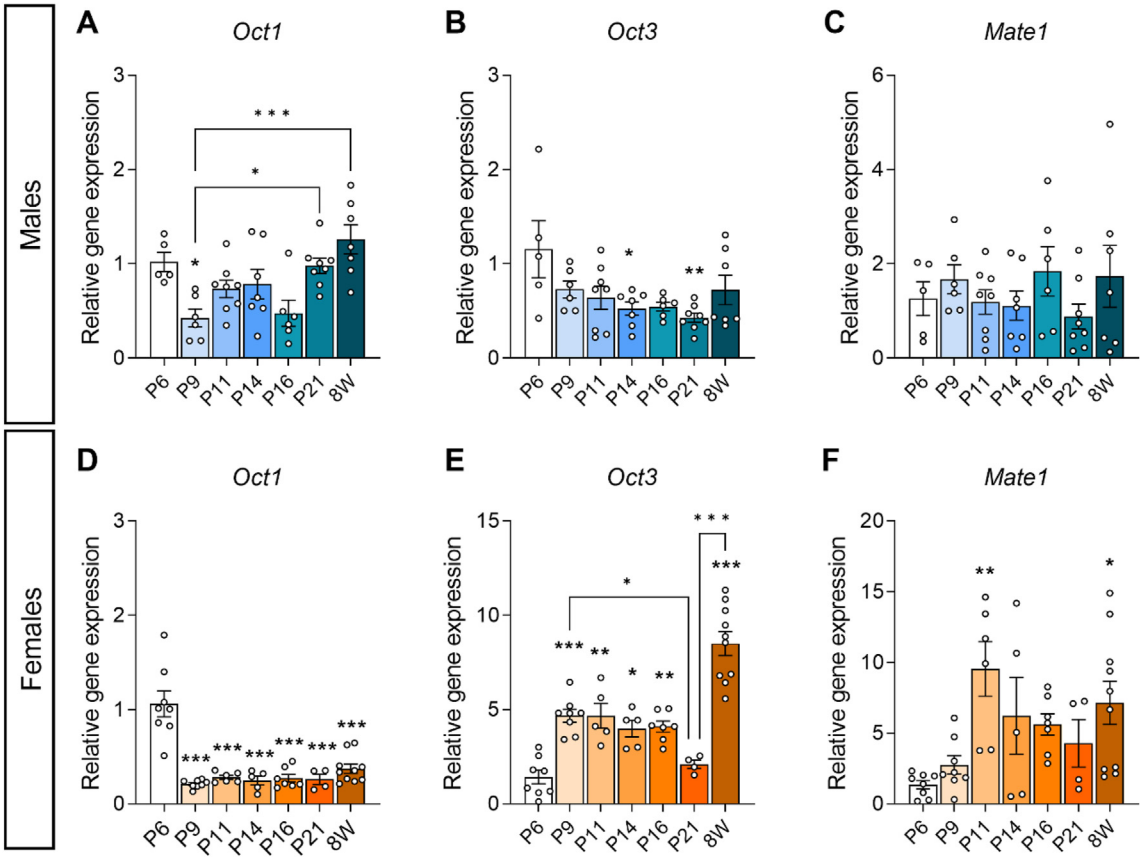

Figure 9: Metformin transporters are expressed in the developing hypothalamus. (A) *Oct1*, (B) *Oct3* and (C) *Mate1* mRNA expression in the hypothalamus across development in wild-type male mice (n = 5–8/time-point). (D) *Oct1*, (E) *Oct3* and (F) *Mate1* mRNA expression in the hypothalamus across development in wild-type female mice (n = 4–10/time-point). Data are expressed as mean ± SEM with single data points in black dots. *p < 0.05, **p < 0.01, ***p < 0.001 compared to P6, unless indicated. P-values derived from one-way ANOVA followed by Tukey's multiple comparisons. P: postnatal day, W: weeks of age.

Table 10 — One-way ANOVA results for Figure 9.

Panel	Source of variation	F (DFn, DFd)	P value
A) *Oct1* in males	Time	F (6, 40) = 5.91	P < 0.001
B) *Oct3* in males	Time	F (6, 40) = 2.94	P = 0.018
C) *Mate1* in males	Time	F (6, 40) = 0.85	P = 0.540
D) *Oct1* in females	Time	F (6, 41) = 19.79	P < 0.001
E) *Oct3* in females	Time	F (6, 40) = 26.27	P < 0.001
F) *Mate1* in females	Time	F (6, 41) = 4.04	P = 0.003

metabolic disorders and obesity in the offspring. Our results showed no significant changes after maternal HFD or metformin treatment in the number of AgRP and POMC neurons in the ARH in P16 offspring, which is in agreement with previous studies [41,42,84]. Interestingly, metformin and insulin treatment led to the most dramatic changes in neuronal projections in both male and female animals in the control diet condition, reiterating that alterations in glucose and insulin homeostasis in development do impact neuronal circuit development. Probing diet and treatment effects, we found a subtle role of maternal overnutrition on AgRP innervation in the PVH. Region-specificity of the effects of maternal HFD were also observed, with the most detrimental effect on the posterior PVH, which is the pre-autonomic compartment, known to regulate pancreatic secretion, adipose storage, thermogenesis and peripheral glucose uptake through its connections to the brainstem [92]. Specifically, male and female animals showed a larger effect on AgRP reduction in the PVHpost, that progressed from P16 to P21 in the maternal GWG group. While metformin does appear to rescue this detriment, in females this results in elevated AgRP signal compared to controls. As it is not known what physiological outcomes are linked to an increase above normal of AgRP innervation, this may be relevant to study further. With regard to α-MSH in this region, males display relatively mild, if any effects, whereas females in the maternal GWG initially show increased projections, which then progress to a decrease by P21 and metformin exposure appears to generate the inverse response, i.e. lower α-MSH projections at P16 and higher at P21 in the CD/HFD group. In line with our findings, postnatal leptin signaling has been shown to impact the axonal terminal densities onto the preautonomic neurons in the PVH [93]. A differential response to anti-diabetic treatments depending on the maternal metabolic state was observed particularly in P21 female offspring, where insulin seems to promote AgRP and α-MSH innervation in offspring of obese mothers, supporting its proposed role as a growth factor in early development [94]. Metformin appears to impair both AgRP and α-MSH fiber densities in control offspring, whereas a promoting effect is observed in offspring of lactating HFD-fed dams. A number of studies in the literature in recent years [41,42,88,95–97] have highlighted effects on neuronal projections relating to maternal diet clearly indicating a role of maternal diet as well as interventions impacting glucose and insulin homeostasis on the development of these neurons. However, the differences in diet, timing, and treatment result in varying effects to AgRP and POMC neuronal innervation in the hypothalamus and

underscore the need for caution when using interventions that will modify the metabolic parameters of the mother.

At a mechanistic level, as AMPK is one of the main molecular targets of metformin and plays a key role in axonal growth during development, we investigated the potential impact of maternal HFD and early metformin exposure on hypothalamic AMPK signaling. We observed an overall reduction in total hypothalamic levels of AMPK induced by maternal HFD in both males and females, although in females the ratio of pAMPK/AMPK was enhanced by maternal HFD. Previous studies showed a reduction in phosphorylated AMPK levels in the developing hypothalamus due to maternal HFD exposure [98,99] and this reduction was attributed to increased insulin and leptin, which are known to inhibit AMPK [100,101]. Although, in our study, we did not detect any change in AMPK activation in response to metformin, this could be related to the fact that higher doses of metformin are required to induce a significant AMPK activation in the hypothalamus, as it is known that metformin-induced AMPK activation is dose-dependent [102]. In addition, the highest peak in AMPK phosphorylation dynamics has been observed 15 min after metformin administration [103]; thus, we might not have been able to detect the acute effects on AMPK activation as the hypothalamus was extracted ~16 h after the last metformin administration. Constitutive AMPK overactivation has also been associated with an impairment of post-synaptic markers in the mouse brain [104], so although we were not able to detect significant changes on the cytoarchitecture of AgRP and POMC neurons after early metformin exposure, alterations on their synaptic connectivity cannot be excluded. An induction of LKB1 by early metformin exposure was detected in P16 females. LKB1, one of the main targets of metformin's action, has been described to regulate neuronal polarity, thus playing a potential role on brain development [105]. In addition, mTOR and ACC, downstream effectors of AMPK signaling were found to be altered by metformin exposure in the hypothalamus of P16 males. Interestingly, hypothalamic mTOR and ACC signaling pathways are involved in food intake regulation [106,107]. Additionally, mTORC1 also regulates axon formation and polarization in the brain [108,109]. As in our study, increased ACC phosphorylation was also found in the liver of P16 male offspring with metformin exposure during lactation [32]. Therefore, early metformin exposure could potentially have an effect on feeding behaviour in males through its modulation of ACC signaling, however, this would need to be further proven in future studies. Overall, the effects seen due to metformin treatment represent a state of suppression of food intake (elevated LKB1 and mTOR for example). However, this immediate effect, while seemingly positive, suppresses food intake and body weight, and may predispose the offspring for elevated rates of weight gain and food intake once metformin is no longer present in circulation. Indeed, studies in older mice assessing alternating weeks of metformin treatment show wide variances in food intake behavior in weeks with or without metformin treatment [110]. Thus, early exposure to metformin as in our studies, show elevated activation of signaling proteins in metformin responsiveness which likely decrease food intake, resulting in the most dramatic reduction in weight gain in the offspring exposed to maternal obesity. However, these offspring may then be predisposed to elevated catch up growth after cessation of treatment. Supporting this is the evidence in humans that elevated rates of weight gain are seen in the children with metformin exposure [86].

4.4. Unique sex-specific effects induced by maternal metabolic state and metformin treatment

Interestingly, our study demonstrates significant sex-specific differences in many of the parameters analysed as previously discussed. Specifically, in females a much stronger elevation in GDF15 in the presence of maternal HFD is noted. Both males and females show an elevation in leptin due to diet, but only males show a normalization with metformin treatment, but here only in the context of maternal obesity. This emphasizes that maternal metabolic state (weight gain versus weight stable) can impact how the offspring respond to metformin treatment. This is also reflected in the glycemic response in which all male animals with metformin exposure show decreased glycemia, independent of which maternal nutritional paradigm. Females with the maternal GWG paradigm do not show decreased glycemia with metformin, indicating again a physiological interaction of maternal metabolic state, sex and treatment. In both sexes, the body weight response to treatment in combination with diet shows striking differences. Indeed, in the context of maternal obesity, a dramatic decrease in body weight gain across the postnatal period is present. However, if the mothers are in a weight gain phase in the GWG model, this effect of treatment on body weight gain is lost, and perhaps even amplifies body weight in the context of treatment. Therefore, it may be critical in human pregnancy to determine the rate of weight gain in comparison to a standardized value, and the intervention of choice (lifestyle, nutritional or pharmaceutical) should be selected accordingly. Previous studies have also shown how early-life environment affects the offspring sexes differently, male offspring being more vulnerable to the obesogenic effects of maternal hyperglycaemia exposure than females [111,112], which might be protected due to the role of ovarian hormones [113]. Furthermore, both clinical and animal studies have reported sex-dependent effects of maternal metformin exposure [32,114,115]. While the underlying mechanism is still unknown, the differential pattern of expression of Octs in the developing hypothalamus between sexes that we show here could be playing a role in the sex differences we reported in our study.

4.5. Conclusions and key points

Metformin usage during pregnancy is becoming more popular, especially in low income and rural areas, due to its relatively low cost and tablet-based route of treatment [116]. Hence, longitudinal studies of metformin exposure at different stages of development are absolutely necessary to understand its long-term effects. This needs to be framed in the context of maternal metabolic state, as we show here clear indications that maternal obesity or maternal excessive weight gain alone result in different effects in the offspring. This in compounded by the fact that dependent on the maternal metabolic state, an interaction with metformin treatment can result in differing outcomes in the offspring. Our study provides evidence that early metformin exposure alters metabolic circulating hormones and induces subtle changes in intrahypothalamic axonal innervation and the AMPK signaling pathway during the early postnatal period. Alterations in hypothalamic structure and function during early life can predispose the offspring to develop metabolic disorders later in life, thus a follow-up analysis into adulthood in mice would help us to understand the long-lasting effects of metformin exposure. A further analysis of cell-type and hypothalamic subregion specificity would be necessary to definitively understand the impact of early metformin exposure in the context of maternal overnutrition. Ultimately, understanding the long-term implications of early developmental exposure to maternal obesity and anti-diabetic treatments, especially those reaching the developing brain, can lead to informed decisions necessary for GDM treatment.

AUTHOR CONTRIBUTIONS

LC and RNL are responsible for experimental design. LC, JZ, SY, BC, JF and RNL conducted all animal work and contributed to tissue

collection. KR performed all genotyping experiments. LC, JZ, SY, LSK, MP, PT and KT contributed to tissue slicing, immunostaining and image analysis. LC, MSL and KR performed RNA extraction, cDNA synthesis and qPCR experiments. LC, MSL and SP performed Western Blot experiments. RC and DBA developed Fiji ImageJ scripts for image analyses. AB performed HPLC analyses. CIG performed GDF-15 measurements. LC and RNL analysed the data and wrote the manuscript. All authors edited and critically reviewed the manuscript. RNL acquired the funding for the project and supervised all authors.

FUNDING

This work was supported financially by the Deutsche Forschungsgemeinschaft under Germany's Excellence Strategy — EXC-2049 — 390688087 (NeuroCure to RNL) and by the German Center for Diabetes Research (82DZD03D2Y and 82DZD03D03 to RNL).

ACKNOWLEDGEMENTS

We would like to acknowledge all of the animal caretaking staff involved in the maintenance and care of the animals in the study. Further, we would like to thank Dr. Susanne Klaus for her support of the project. We would also like to thank Dr. Jens Brüning for sharing the POMC-Cre, AgRP-Cre and Synaptophysin-Tdtomato mouse lines.

DECLARATION OF COMPETING INTEREST

The authors declare that they have no known competing financial interests or personal relationships that could have appeared to influence the work reported in this paper.

DATA AVAILABILITY

Data will be made available on request.

APPENDIX A. SUPPLEMENTARY DATA

Supplementary data to this article can be found online at https://doi.org/10.1016/j.molmet.2023.101860.

REFERENCES

[1] Wang H, Li N, Chivese T, Werfalli M, Sun H, Yuen L, et al. IDF diabetes atlas: estimation of global and regional gestational diabetes mellitus prevalence for 2021 by international association of diabetes in pregnancy study group's criteria. Diabetes Res Clin Pract 2022;183:109050.

[2] Paulo MS, Abdo NM, Bettencourt-Silva R, Al-Rifai RH. Gestational diabetes mellitus in europe: a systematic review and meta-analysis of prevalence studies. Front Endocrinol 2021;12:691033.

[3] Reitzle L, Schmidt C, Heidemann C, Icks A, Kaltheuner M, Ziese T, et al. Gestational diabetes in Germany: development of screening participation and prevalence. Journal of Health Monitoring 2021;6(2):3—18.

[4] Saravanan P, Magee LA, Banerjee A, Coleman MA, Von Dadelszen P, Denison F, et al. Gestational diabetes: opportunities for improving maternal and child health. Lancet Diabetes Endocrinol 2020:793—800.

[5] Lowe WL, Scholtens DM, Kuang A, Linder B, Lawrence JM, Lebenthal Y, et al. Hyperglycemia and adverse Pregnancy Outcome follow-up study (HAPO FUS): maternal gestational diabetes mellitus and childhood glucose metabolism. Diabetes Care 2019;42(3):372—80.

[6] Lowe WL, Lowe LP, Kuang A, Catalano PM, Nodzenski M, Talbot O, et al. Maternal glucose levels during pregnancy and childhood adiposity in the hyperglycemia and adverse pregnancy outcome follow-up study. Diabetologia 2019;62(4):598—610.

[7] McIntyre HD, Catalano P, Zhang C, Desoye G, Mathiesen ER, Damm P. Gestational diabetes mellitus. Nat Rev Dis Prim 2019;5(1):47.

[8] Pollex EK, Feig DS, Lubetsky A, Yip PM, Koren G. Insulin glargine safety in pregnancy: a transplacental transfer study. Diabetes Care 2010;33(1):29—33.

[9] Suffecool K, Rosenn B, Niederkofler EE, Kiernan UA, Foroutan J, Antwi K, et al. Insulin detemir does not cross the human placenta. Diabetes Care 2015:e20—1.

[10] Yu Y, Platt RW, Reynier P, Yu OHY, Filion KB. Use of metformin and insulin among pregnant women with gestation diabetes in the United Kingdom: a population-based cohort study. Diabet Med 2023;40(8):e15108.

[11] National Institute for Health and Care Excellence. Diabetes in pregnancy: management from preconception to the postnatal period NICE guideline [NG3]. 2015. https://www.nice.org.uk/guidance/ng3.

[12] Schäfer-Graf U, Gembruch U, Kainer F, Groten T, Hummel S, Hösli I, et al. Gestational diabetes mellitus (GDM) — diagnosis, treatment and follow-up. Guideline of the DDG and DGGG (S3 level, AWMF registry number 057/008, february 2018). Geburtshilfe Frauenheilkd 2018;78(12):1219—31.

[13] van Weelden W, Wekker V, de Wit L, Limpens J, Ijäs H, van Wassenaer-Leemhuis AG, et al. Long-term effects of oral antidiabetic drugs during pregnancy on offspring: a systematic review and meta-analysis of follow-up studies of RCTs. Diabetes Therapy : Research, Treatment and Education of Diabetes and Related Disorders 2018;9(5):1811—29.

[14] Dunne F, Newman C, Alvarez-Iglesias A, Ferguson J, Smyth A, Browne M, et al. Early metformin in gestational diabetes. JAMA 2023;330(16):1547—56.

[15] Vanky E, Zahlsen K, Spigset O, Carlsen SM. Placental passage of metformin in women with polycystic ovary syndrome. Fertil Steril 2005;83(5):1575—8.

[16] Ahmadimoghaddam D, Staud F. Transfer of metformin across the rat placenta is mediated by organic cation transporter 3 (OCT3/SLC22A3) and multidrug and toxin extrusion 1 (MATE1/SLC47A1) protein. Reprod Toxicol 2013;39:17—22.

[17] Rowan JA, Rush EC, Obolonkin V, Battin M, Wouldes T, Hague WM. Metformin in gestational diabetes: the offspring follow-up (MiG TOFU): body composition at 2 years of age. Diabetes Care 2011;34(10):2279—84.

[18] Rowan JA, Rush EC, Plank LD, Lu J, Obolonkin V, Coat S, et al. Metformin in gestational diabetes: the offspring follow-up (MiG TOFU): body composition and metabolic outcomes at 7—9 years of age. BMJ Open Diabetes Research & Care 2018;6(1):e000456.

[19] Rowan JA, Rush EC, Plank LD. Metformin in Gestational Diabetes the Offspring Follow up (MiGTOFU): associations between maternal characteristics and size and adiposity of boys and girls at nine years. Aust N Z J Obstet Gynaecol 2023;63(6):825—8.

[20] Paavilainen E, Tertti K, Nikkinen H, Veijola R, Vääräsmäki M, Loo B-M, et al. Metformin versus insulin therapy for gestational diabetes: effects on offspring anthropometrics and metabolism at the age of 9 years: a follow-up study of two open-label, randomized controlled trials. Diabetes Obes Metabol 2022;24(3):402—10.

[21] Paavilainen E, Niinikoski H, Parkkola R, Koskensalo K, Nikkinen H, Veijola R, et al. Metformin versus insulin for gestational diabetes: adiposity variables and adipocytokines in offspring at age of 9 years. Diabetes Res Clin Pract 2023;202:110780.

[22] Hanem LGE, Stridsklev S, Júlíusson PB, Salvesen Ø, Roelants M, Carlsen SM, et al. Metformin use in PCOS pregnancies increases the risk of offspring overweight at 4 Years of age: follow-up of two RCTs. J Clin Endocrinol Metabol 2018;103(4):1612—21.

[23] Fornes R, Simin J, Nguyen MH, Cruz G, Crisosto N, van der Schaaf M, et al. Pregnancy, perinatal and childhood outcomes in women with and without polycystic ovary syndrome and metformin during pregnancy: a nationwide population-based study. Reprod Biol Endocrinol 2022;20(1):30.
[24] Brand KMG, Saarelainen L, Sonajalg J, Boutmy E, Foch C, Vääräsmäki M, et al. Metformin in pregnancy and risk of adverse long-term outcomes: a register-based cohort study. BMJ Open Diabetes Research & Care 2022;10(1):e002363.
[25] Tocci V, Mirabelli M, Salatino A, Sicilia L, Giuliano S, Brunetti FS, et al. Metformin in gestational diabetes mellitus: to use or not to use, that is the question. Pharmaceuticals 2023;16(9):1318.
[26] Paschou SA, Shalit A, Gerontiti E, Athanasiadou KI, Kalampokas T, Psaltopoulou T, et al. Efficacy and safety of metformin during pregnancy: an update. Endocrine 2023:1–11.
[27] Salomäki H, Vähätalo LH, Laurila K, Jäppinen NT, Penttinen A-M, Ailanen L, et al. Prenatal metformin exposure in mice programs the metabolic phenotype of the offspring during a high fat diet at adulthood. PLoS One 2013;8(2):e56594.
[28] Salomäki H, Heinäniemi M, Vähätalo LH, Ailanen L, Eerola K, Ruohonen ST, et al. Prenatal metformin exposure in a maternal high fat diet mouse model alters the transcriptome and modifies the metabolic responses of the offspring. PLoS One 2014;9(12):e115778.
[29] Schoonejans JM, Blackmore HL, Ashmore TJ, Aiken CE, Fernandez-Twinn DS, Ozanne SE. Maternal metformin intervention during obese glucose-intolerant pregnancy affects adiposity in young adult mouse offspring in a sex-specific manner. Int J Mol Sci 2021;22(15):8104.
[30] Hufnagel A, Fernandez-Twinn DS, Blackmore HL, Ashmore TJ, Heaton RA, Jenkins B, et al. Maternal but not fetoplacental health can be improved by metformin in a murine diet-induced model of maternal obesity and glucose intolerance. J Physiol 2022;600(4):903–19.
[31] Gregg BE, Botezatu N, Brill JD, Hafner H, Vadrevu S, Satin LS, et al. Gestational exposure to metformin programs improved glucose tolerance and insulin secretion in adult male mouse offspring. Sci Rep 2018;8(1):1–11.
[32] Carlson Z, Hafner H, Mulcahy M, Bullock K, Zhu A, Bridges D, et al. Lactational metformin exposure programs offspring white adipose tissue glucose homeostasis and resilience to metabolic stress in a sex-dependent manner. Am J Physiol Endocrinol Metabol 2020;318(5):E600–12.
[33] Hafner H, Mulcahy MC, Carlson Z, Hartley P, Sun H, Westerhoff M, et al. Lactational high fat diet in mice causes insulin resistance and NAFLD in male offspring which is partially rescued by maternal metformin treatment. Front Nutr 2021;8:951.
[34] Carlson Z, Hafner H, Habbal N El, Harman E, Liu S, Botezatu N, et al. Short term changes in dietary fat content and metformin treatment during lactation impact milk composition and mammary gland morphology. J Mammary Gland Biol Neoplasia 2022;27(1):1–18.
[35] Amato S, Liu X, Zheng B, Cantley L, Rakic P, Man HY. AMP-activated protein kinase regulates neuronal polarization by interfering with PI 3-kinase localization. Science 2011;332(6026):247–51.
[36] Ramamurthy S, Chang E, Cao Y, Zhu J, Ronnett GV. AMPK activation regulates neuronal structure in developing hippocampal neurons. Neuroscience 2014;259:13–24.
[37] Williams T, Courchet J, Viollet B, Brenman JE, Polleux F. AMP-activated protein kinase (AMPK) activity is not required for neuronal development but regulates axogenesis during metabolic stress. Proc Natl Acad Sci USA 2011;108(14):5849–54.
[38] Bouret SG, Draper SJ, Simerly RB. Formation of projection pathways from the arcuate nucleus of the hypothalamus to hypothalamic regions implicated in the neural control of feeding behavior in mice. J Neurosci 2004;24(11):2797–805.
[39] Steculorum SM, Vogt MC, Brüning JC. Perinatal programming of metabolic diseases. Role of insulin in the development of hypothalamic neurocircuits. Endocrinology and Metabolism Clinics of North America; 2013. p. 149–64.
[40] Lippert RN, Brüning JC. Maternal metabolic programming of the developing central nervous system: unified pathways to metabolic and psychiatric disorders. Biol Psychiatr 2022;91(10):898–906.
[41] Vogt MC, Paeger L, Hess S, Steculorum SM, Awazawa M, Hampel B, et al. Neonatal insulin action impairs hypothalamic neurocircuit formation in response to maternal high-fat feeding. Cell 2014;156(3):495–509.
[42] Park S, Jang A, Bouret SG. Maternal obesity-induced endoplasmic reticulum stress causes metabolic alterations and abnormal hypothalamic development in the offspring. PLoS Biol 2020;18(3):e3000296.
[43] Claret M, Smith MA, Batterham RL, Selman C, Choudhury AI, Fryer LGD, et al. AMPK is essential for energy homeostasis regulation and glucose sensing by POMC and AgRP neurons. J Clin Invest 2007;117(8):2325–36.
[44] Page KA, Luo S, Wang X, Chow T, Alves J, Buchanan TA, et al. Children exposed to maternal obesity or gestational diabetes mellitus during early fetal development have hypothalamic alterations that predict future weight gain. Diabetes Care 2019;42(8):1473–80.
[45] Rasmussen JM, Thompson PM, Gyllenhammer LE, Lindsay KL, O'Connor TG, Koletzko B, et al. Maternal free fatty acid concentration during pregnancy is associated with newborn hypothalamic microstructure in humans. Obesity 2022;30(7):1462–71.
[46] Magon N, Seshiah V. Gestational diabetes mellitus: insulinic management. J Obstet Gynaecol India 2014;64(2):82–90.
[47] Reagan-Shaw S, Nihal M, Ahmad N. Dose translation from animal to human studies revisited. FASEB (Fed Am Soc Exp Biol) J : Official Publication of the Federation of American Societies for Experimental Biology 2008;22(3):659–61.
[48] Chhetri HP, Thapa P, Van Schepdael A. Simple HPLC-UV method for the quantification of metformin in human plasma with one step protein precipitation. Saudi Pharmaceut J 2014;22(5):483–7.
[49] Metzger BE, Gabbe SG, Persson B, Buchanan TA, Catalano PA, Damm P, et al. International association of diabetes and pregnancy study groups recommendations on the diagnosis and classification of hyperglycemia in pregnancy. Diabetes Care 2010;33(3):676–82.
[50] Semple BD, Blomgren K, Gimlin K, Ferriero DM, Noble-Haeusslein LJ. Brain development in rodents and humans: identifying benchmarks of maturation and vulnerability to injury across species. Prog Neurobiol 2013;106–107(Jul-Aug):1–16.
[51] Gerstein HC, Pare G, Hess S, Ford RJ, Sjaarda J, Raman K, et al. Growth differentiation factor 15 as a novel biomarker for metformin. Diabetes Care 2017;40(2):280–3.
[52] LaMoia TE, Shulman GI. Cellular and molecular mechanisms of metformin action. Endocr Rev 2021;42(1):77–96.
[53] Briggs GG, Ambrose PJ, Nageotte MP, Padilla G, Wan S. Excretion of metformin into breast milk and the effect on nursing infants. Obstet Gynecol 2005;105(6):1437–41.
[54] Gardiner S. Transfer of metformin into human milk. Clin Pharmacol Therapeut 2003;73(1):71–7.
[55] Eyal S, Easterling TR, Carr D, Umans JG, Miodovnik M, Hankins GDV, et al. Pharmacokinetics of metformin during pregnancy. Drug Metabol Dispos 2010;38(5):833–40.
[56] Wang L, Cai Y, Fan X. Metformin administration during early postnatal life rescues autistic-like behaviors in the BTBR T+ Itpr3tf/J mouse model of autism. Front Behav Neurosci 2018;12:290.
[57] König B, Markl H. Maternal care in house mice: I. The weaning Strategy as a means for parental manipulation of offspring quality. Behav Ecol Sociobiol 1987;20:1–9.

[58] Díaz M, Campderrós L, Guimaraes MP, López-Bermejo A, de Zegher F, Villarroya F, et al. Circulating growth-and-differentiation factor-15 in early life: relation to prenatal and postnatal growth and adiposity measurements. Pediatr Res 2020;87(5):897—902.
[59] Ruddy RM, Adams KV, Morshead CM. Age- and sex-dependent effects of metformin on neural precursor cells and cognitive recovery in a model of neonatal stroke. Sci Adv 2019;5(9).
[60] Woods A, Johnstone SR, Dickerson K, Leiper FC, Fryer LGD, Neumann D, et al. LKB1 is the upstream kinase in the AMP-activated protein kinase cascade. Curr Biol : CB 2003;13(22):2004—8.
[61] Nakano A, Takashima S. LKB1 and AMP-activated protein kinase: regulators of cell polarity. Gene Cell 2012:737—47.
[62] Shaw RJ, Lamia KA, Vasquez D, Koo S-H, Bardeesy N, Depinho RA, et al. The kinase LKB1 mediates glucose homeostasis in liver and therapeutic effects of metformin. Science (New York, N.Y.) 2005;310(5754):1642—6.
[63] Gwinn DM, Shackelford DB, Egan DF, Mihaylova MM, Mery A, Vasquez DS, et al. AMPK phosphorylation of raptor mediates a metabolic checkpoint. Mol Cell 2008;30(2):214—26.
[64] Howell JJ, Hellberg K, Turner M, Talbott G, Kolar MJ, Ross DS, et al. Metformin inhibits hepatic mTORC1 signaling via dose-dependent mechanisms involving AMPK and the TSC complex. Cell Metabol 2017;25(2):463—71.
[65] Zhou G, Myers R, Li Y, Chen Y, Shen X, Fenyk-Melody J, et al. Role of AMP-activated protein kinase in mechanism of metformin action. J Clin Invest 2001;108(8):1167—74.
[66] Couroussé T, Gautron S. Role of organic cation transporters (OCTs) in the brain. Pharmacol Therapeut 2015;146:94—103.
[67] Sharma S, Zhang Y, Akter KA, Nozohouri S, Archie SR, Patel D, et al. Permeability of metformin across an in vitro blood—brain barrier model during normoxia and oxygen-glucose deprivation conditions: role of organic cation transporters (Octs). Pharmaceutics 2023;15(5):1357.
[68] Lee H, Lee Y, Kim J, An J, Lee S, Kong H, et al. Modulation of the gut microbiota by metformin improves metabolic profiles in aged obese mice. Gut Microb 2018;9(2):155—65.
[69] Goldstein RF, Abell SK, Ranasinha S, Misso M, Boyle JA, Black MH, et al. Association of gestational weight gain with maternal and infant outcomes: a systematic review and meta-analysis. JAMA 2017;317(21):2207—25.
[70] Yang H, Chen N, Fan L, Lin X, Liu J, You Y, et al. Pre-weaning exposure to maternal high-fat diet is a critical developmental window for programming the metabolic system of offspring in mice. Front Endocrinol 2022;13:816107.
[71] Torres-Espinola FJ, Berglund SK, García-Valdés LM, Segura MT, Jerez A, Campos D, et al. Maternal obesity, overweight and gestational diabetes affect the offspring neurodevelopment at 6 and 18 Months of age — a follow up from the preobe cohort. PLoS One 2015;10(7):e0133010.
[72] Aubert G, Mansuy V, Voirol M-J, Pellerin L, Pralong FP. The anorexigenic effects of metformin involve increases in hypothalamic leptin receptor expression. Metabolism 2011;60(3):327—34.
[73] Lv WS, Wen JP, Li L, Sun RX, Wang J, Xian YX, et al. The effect of metformin on food intake and its potential role in hypothalamic regulation in obese diabetic rats. Brain Res 2012;1444:11—9.
[74] Duan Y, Zhang R, Zhang M, Sun LJ, Dong SZ, Wang G, et al. Metformin inhibits food intake and neuropeptide Y gene expression in the hypothalamus. Neural Regeneration Research 2013;8(25):2379—88.
[75] Schultes B, Oltmanns KM, Kern W, Fehm HL, Born J, Peters A. Modulation of hunger by plasma glucose and metformin. J Clin Endocrinol Metabol 2003;88(3):1133—41.
[76] Kinaan M, Ding H, Triggle CR. Metformin: an old drug for the treatment of diabetes but a new drug for the protection of the endothelium. Med Princ Pract 2015;24(5):401—15.
[77] Goldman J, White JR. Advances in basal insulin therapy. J Pharm Technol 2016;32(6):260—8.
[78] Chiswick C, Reynolds RM, Denison F, Drake AJ, Forbes S, Newby DE, et al. Effect of metformin on maternal and fetal outcomes in obese pregnant women (EMPOWaR): a randomised, double-blind, placebo-controlled trial. The Lancet. Diabetes & Endocrinology 2015;3(10):778.
[79] Sharma N, Siriesha, Lugani Y, Kaur A, Ahuja VK. Effect of metformin on insulin levels, blood sugar, and body mass index in polycystic ovarian syndrome cases. J Fam Med Prim Care 2019;8(8):2691.
[80] Wang Y, An H, Liu T, Qin C, Sesaki H, Guo S, et al. Metformin improves mitochondrial respiratory activity through activation of AMPK. Cell Rep 2019;29(6):1511—1523.e5.
[81] Coll AP, Chen M, Taskar P, Rimmington D, Patel S, Tadross JA, et al. GDF15 mediates the effects of metformin on body weight and energy balance. Nature 2020;578(7795):444—8.
[82] Day EA, Ford RJ, Smith BK, Mohammadi-Shemirani P, Morrow MR, Gutgesell RM, et al. Metformin-induced increases in GDF15 are important for suppressing appetite and promoting weight loss. Nat Metab 2019:1202—8.
[83] Priya G, Kalra S. Metformin in the management of diabetes during pregnancy and lactation. Drugs Context (US) 2018;7:1—21.
[84] Haddad-Tóvolli R, Altirriba J, Obri A, Sánchez EE, Chivite I, Milà-Guasch M, et al. Pro-opiomelanocortin (POMC) neuron translatome signatures underlying obesogenic gestational malprogramming in mice. Mol Metabol 2020;36:100963.
[85] Perichart-Perera O, Rodríguez-Cano AM, González-Ludlow I, Rodríguez-Hernández C, Suárez-Rico B, Reyes-Muñoz E, et al. Gestational diabetes mellitus and size at birth modify early adiposity accretion. Evidence from the OBESO cohort. Diabetes Research and Clinical Practice; 2023. p. 110889.
[86] Tarry-Adkins JL, Aiken CE, Ozanne SE. Neonatal, infant, and childhood growth following metformin versus insulin treatment for gestational diabetes: a systematic review and meta-analysis. PLoS Med 2019;16(8):e1002848.
[87] Gawlińska K, Gawliński D, Borczyk M, Korostyński M, Przegaliński E, Filip M. A maternal high-fat diet during early development provokes molecular changes related to autism spectrum disorder in the rat offspring brain. Nutrients 2021;13(9).
[88] Kirk SL, Samuelsson AM, Argenton M, Dhonye H, Kalamatianos T, Poston L, et al. Maternal obesity induced by diet in rats permanently influences central processes regulating food intake in offspring. PLoS One 2009;4(6):5870.
[89] Cui J, Song L, Wang R, Hu S, Yang Z, Zhang Z, et al. Maternal metformin treatment during gestation and lactation improves skeletal muscle development in offspring of rat dams fed high-fat diet. Nutrients 2021;13(10):3417.
[90] Gagnon J, Sheppard E, Anini Y. Metformin directly inhibits ghrelin secretion through AMP-activated protein kinase in rat primary gastric cells. Diabetes Obes Metabol 2013;15(3):276—9.
[91] Rø TB, Ludvigsen HV, Carlsen SM, Vanky E. Growth, body composition and metabolic profile of 8-year-old children exposed to metformin in utero. Scand J Clin Lab Investig 2012;72(7):570—5.
[92] Geerling JC, Shin J-W, Chimenti PC, Loewy AD. Paraventricular hypothalamic nucleus: axonal projections to the brainstem. J Comp Neurol 2010;518(9):1460—99.
[93] Bouyer K, Simerly RB. Neonatal leptin exposure specifies innervation of presympathetic hypothalamic neurons and improves the metabolic status of leptin-deficient mice. J Neurosci 2013;33(2):840—51.
[94] Yagoub S, Lippert RN. Insulin/IGF signaling in early brain development. In: Physiological consequences of brain insulin action. CRC Press; 2022. p. 21—33.
[95] Song L, Cui J, Wang R, Wang N, Yan J, Sun B. Maternal exercise and high-fat diet affect hypothalamic neural projections in rat offspring in a sex-specific manner. J Nutr Biochem 2022;103:108958.
[96] Steculorum SM, Bouret SG. Maternal diabetes compromises the organization of hypothalamic feeding circuits and impairs leptin sensitivity in offspring. Endocrinology 2011;152(11):4171.

[97] Haddad-Tóvolli R, Morari J, Barbizan R, Bóbbo VC, Carraro RS, Solon C, et al. Maternal obesity damages the median eminence blood-brain barrier structure and function in the progeny: the beneficial impact of cross-fostering by lean mothers. Am J Physiol Endocrinol Metabol 2023;324(2): E154–66.

[98] Desai M, Ferrini MG, Han G, Narwani K, Ross MG. Maternal high fat diet programs male mice offspring hyperphagia and obesity: mechanism of increased appetite neurons via altered neurogenic factors and nutrient sensor ampk. Nutrients 2020;12(11):1–17.

[99] Bae-Gartz I, Janoschek R, Breuer S, Schmitz L, Hoffmann T, Ferrari N, et al. Maternal obesity alters neurotrophin-associated MAPK signaling in the hypothalamus of male mouse offspring. Front Neurosci 2019;13:962.

[100] Andersson U, Filipsson K, Abbott CR, Woods A, Smith K, Bloom SR, et al. AMP-Activated protein kinase plays a role in the control of food intake. J Biol Chem 2004;279(13):12005–8.

[101] Minokoshi Y, Alquier T, Furukawa H, Kim YB, Lee A, Xue B, et al. AMP-kinase regulates food intake by responding to hormonal and nutrient signals in the hypothalamus. Nature 2004;428(6982):569–74.

[102] Hawley SA, Gadalla AE, Olsen GS, Hardie DG. The antidiabetic drug metformin activates the AMP-activated protein kinase cascade via an adenine nucleotide-independent mechanism. Diabetes 2002;51(8):2420–5.

[103] Demaré S, Kothari A, Calcutt NA, Fernyhough P. Metformin as a potential therapeutic for neurological disease: mobilizing AMPK to repair the nervous system. Expert Rev Neurother 2021;21(1):45–63.

[104] Domise M, Sauvé F, Didier S, Caillerez R, Bégard S, Carrier S, et al. Neuronal AMP-activated protein kinase hyper-activation induces synaptic loss by an autophagy-mediated process. Cell Death Dis 2019;10(3):221.

[105] Kuwako K, Okano H. Versatile roles of LKB1 kinase signaling in neural development and homeostasis. Front Mol Neurosci 2018;11:354.

[106] Cota D, Proulx K, Smith KAB, Kozma SC, Thomas G, Woods SC, et al. Hypothalamic mTOR signaling regulates food intake. Science 2006;312(5775): 927–30.

[107] Xue B, Kahn BB. AMPK integrates nutrient and hormonal signals to regulate food intake and energy balance through effects in the hypothalamus and peripheral tissues. J Physiol 2006;574(1):73–83.

[108] Li YH, Werner H, Püschel AW. Rheb and mTOR regulate neuronal polarity through Rap1B. J Biol Chem 2008;283(48):33784.

[109] Choi YJ, Di Nardo A, Kramvis I, Meikle L, Kwiatkowski DJ, Sahin M, et al. Tuberous sclerosis complex proteins control axon formation. Gene Dev 2008;22(18):2485–95.

[110] Alfaras I, Mitchell SJ, Mora H, Lugo DR, Warren A, Navas-Enamorado I, et al. Health benefits of late-onset metformin treatment every other week in mice. Npj Aging and Mechanisms of Disease 2017;3(1):16.

[111] Lu Y, Jia Y, Lu J, Liu J, Xu Y, Liu Y, et al. Progenies of gestational diabetes mellitus exhibit sex disparity in metabolism after respective therapies of insulin, glibenclamide, and metformin in dams during pregnancy. Arch Physiol Biochem 2021:1–13.

[112] Dearden L, Bouret SG, Ozanne SE. Sex and gender differences in developmental programming of metabolism. Mol Metabol 2018;15:8–19.

[113] Tramunt B, Smati S, Grandgeorge N, Lenfant F, Arnal JF, Montagner A, et al. Sex differences in metabolic regulation and diabetes susceptibility. Diabetologia 2020;63(3):453–61.

[114] Schoonejans JM, Blackmore HL, Ashmore TJ, Pantaleão LC, Pellegrini Pisani L, Dearden L, et al. Sex-specific effects of maternal metformin intervention during glucose-intolerant obese pregnancy on body composition and metabolic health in aged mouse offspring. Diabetologia 2022;65(12): 2132–45.

[115] Garcia-Contreras C, Vazquez-Gomez M, Pesantez-Pacheco J, Heras-Molina A, Encinas T, Astiz S, et al. The effects of maternal metformin treatment on late prenatal and early postnatal development of the offspring are modulated by sex. Pharmaceuticals 2020;13(11):363.

[116] Kattini R, Kelly L, Hummelen R. Systematic review of the use of metformin compared to insulin for the management of gestational diabetes: implications for low-resource settings. Can J Rural Med 2023;28(2):59.

